Graduate Dissertations and Theses

Dissertations, Theses and Capstones

5-3-2018

Quantifying Factors That Influence Road Deicer Retention and Export in a Multi-Landuse Upstate New York Watershed

David Joseph Saba

Binghamton University--SUNY, dsaba1@binghamton.edu

Recommended Citation

QUANTIFYING FACTORS THAT INFLUENCE ROAD DEICER RETENTION AND
EXPORT IN A MULTI-LANDUSE UPSTATE NEW YORK WATERSHED

BY

DAVID JOSEPH SABA

BS, University at Buffalo State University of New York, 2014

THESIS

Submitted in partial fulfillment of the requirements for
the degree of Master of Science in Geology
in the Graduate School of
Binghamton University
State University of New York
2018

Accepted in partial fulfillment of the requirements for
the degree of Masters of Science in Geology
in the Graduate School of
Binghamton University
State University of New York
2018

May 3, 2018

Dr. Joseph Graney, Faculty Advisor
Department of Geological Sciences and Environmental Studies,
Binghamton University

Dr. Robert Demicco, Committee Member
Department of Geological Sciences and Environmental Studies,
Binghamton University

Dr. Thomas Kulp, Committee Member
Department of Geological Sciences and Environmental Studies,
Binghamton University

Abstract

Chloride contamination of streams and groundwater has become a prevalent issue throughout urbanizing areas in the last half century, particularly in northern latitudes where deicing salts are applied to roadways. This study determined how deicer impacted runoff disperses through sub-urban and urban areas on seasonal and multi-year scales. Chloride concentration changes were then modelled under varying pollutant loading scenarios through an integrated catchment model (INCA-Cl).

Six in-stream conductivity/stage/temperature sondes, recording at 15-minute intervals, were installed within the small (~9.6 km^2) Fuler Hollow Creek multi-landuse watershed in Broome County NY and monitored over a 1-year period. Weekly grab samples were taken at each sonde site and analyzed for dissolved cations and anions to help interpret the sensor results. Data from these sensors and local weather stations were used as inputs to the INCA-Cl model. Conductivity and Discharge measurements from stream sondes were used to construct a concentration/discharge hysteresis model of six storm events to determine seasonal variability in stream pollutant source. Results from weekly Fall and Spring stream and groundwater grab samples from 2006-2016 were used in conjunction with the model results to interpret long term trends.

Stream response to storm events was found to be dependent on season as well as amount of impervious surface. In contrast to the urban locations, sub-urban sites did not have an initial increase in total dissolved solids (TDS) before dilution during summer and fall runoff events and had overall smaller TDS increases from winter and spring de-icer flushing events, as well as slower discharge response times. TDS of stream water within the watershed showed increasing concentrations over the 10-year period that cannot be solely accounted for by an increase in

impervious surface, thus suggesting an accumulation of deicers in groundwater as well. These observations are consistent with seasonal cation and anion data which suggests baseflow composition retains elevated de-icer levels year-round in parts of the watershed.

Concentration/Discharge (C/Q) hysteresis models indicate groundwater is the dominant pollutant source in non-salting seasons compared to surface water being the dominant source in salting seasons. Response to storm events was also influenced by land use in addition to season. INCA-Cl was able to model seasonal discharge and chloride trends within Fuller Hollow Creek under variable loading conditions throughout the study period. However, chloride increases from individual deicer flushing events could not be accurately replicated with the model. By quantifying and understanding the effects of road salting practices on variable land use areas, better estimates of chloride export and retention can be developed in order to protect salt sensitive freshwater ecosystems.

Acknowledgements

Table of Contents

List of Tables

List of Figures

Chapter 1 - Introduction

Since the mid-20th century the use of road deicers has been commonplace within the

northern United States. The most commonly used, and cost-effective, road deicing agent is

sodium chloride (NaCl). Deicing agents applied to road surfaces can create a brine solution upon

contact with snow or water. These solutions can form at sub-zero Celsius temperatures and

prevent buildup of snow on road surfaces or create an aqueous layer between the snow and

road surface that enables easier snow removal. Road salting practices have been shown to

greatly reduce traffic accidents, with pre-salting accident rates 8 times higher on two lane roads

and 4.5 times higher on multilane freeways when compared to post icing conditions (Kuemmel

et. al 1992).
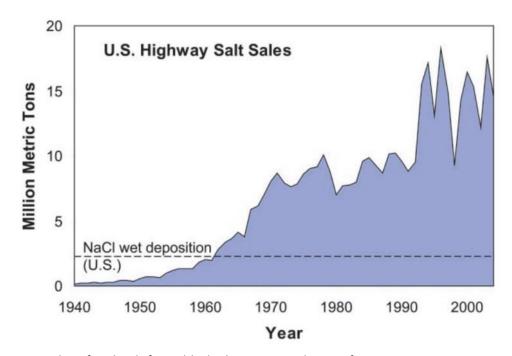
Figure 1.0- Sales of rock salt for public highway use in the U.S. from 1940-2004. Wet
atmospheric NaCl deposition taken from 1999-2003 data. (Jackson and Jobbagy, 2005)

In the United States over 15-18 million metric tons of road salt per year are applied to public roads (Figure 1.1), most of which is applied to urban areas. Despite these benefits, deicer contamination of urban streams and reservoirs has become a prevalent issue throughout urbanizing areas in the last half century (Daley et. al 2009, Jin et. al 2011, Shaw et. al 2012); particularly in northern latitudes where the use of road salts is the primary source of this contamination (Kelly et. al 2007, Mullaney et. al 2009, Gutchess et. al 2016).

Runoff from urban surfaces can be characterized as both a non-point pollution source, as well as a conduit for these contaminants to directly enter surface waters by bypassing natural biological or geological filters (Lee et. al 2000, Zhu et. al 2008, Ledford et. al 2016). As the importance of natural riparian buffers becomes more widely recognized as a way to mitigate levels of dissolved solids, sediment loads, and rates of erosion, more emphasis has been placed on preserving and promoting these buffers. Chronic elevated levels of NaCl in streams have been found to be toxic to aquatic organisms, increase organism susceptibility to pathogens, and harm aquatic and riparian vegetation (Daley et. al 2009, NRC 1991).

Chloride makes an ideal ion for analysis of quantification of road salting pollution due to its conservative nature (Kelly 2008). While dissolved sodium may represent 50 mole percent of the initial road salt pollutants, much is thought to be retained in soils by means of cation exchange resulting in molar Na^+/Cl^- ratios in contaminated urban streams ranging between ~1/1 to ~1/2 (Mullaney et. al 2009, Jin et al. 2011, Kelly et al. 2007). Chloride was also selected as a target ion in this study due to its toxicity to aquatic organisms and potential human health hazard as increasing concentrations may mobilize toxic metals in soils and water infrastructure (Kaushal 2016).

Large amounts of sodium have also been shown to displace nutrients in soil and ground water through cation exchange; this may result in the release of potassium, magnesium, calcium, and other metals, creating conditions toxic to native species (Amrhein et. al 1992, Kaushal et. al 2017). Additionally, sodium exchange with soil organic matter causes a significant reduction in soil permeability, thus increasing erosion and direct runoff to streams leading to higher contaminant concentrations in surface waters (Amrhein et. al 1992).

In many instances, the effects of road salting on streams are not only present in winter months, but year-round due to elevated chloride levels in baseflow from the long-term accumulation of these contaminants in groundwater (Corsi et. al 2015, Kelly et. al 2007, Novotny et. al 2009, Sun et.al 2012). This long-term accumulation also makes chloride contamination a human health issue, particularly for those who rely on unregulated private wells for drinking water (Daley et. al 2009). This is particularly true for much of the northern United States and Canada, which heavily relies on the glacial aquifer system for private and municipal drinking water (Mullaney et. al 2009). This shallow aquifer system is often highly interconnected with surface waters which may contribute to a degradation of surficial water quality. Long term studies on watersheds exposed to road salting practices have concluded that chloride concentrations steadily increase over time, even in areas with no net increase in urbanization, suggesting salts can be accumulated in groundwater; therefore, sustained road salting practices may have serious implications regarding the fate of aquatic and riparian ecosystems and access to potable groundwater (Kelly et. al 2007, Daley et. al 2009, Fay and Shi 2012)

1.1 Study Area

The Fuller Hollow Creek watershed is a small (9.6km^2) watershed in Brome County NY, located within the Upper Appalachian Plateau (Figure 1.1.1). Soil types within the Fuller Hollow

Creek Watershed are heavily influenced by the last glaciation, which peaked about 23kya. Valley

floor sediments within the Glaciated Appalachian Plateau region are primarily comprised of

glacial outwash, as well as alluvium from active stream channels; whereas soils of valley walls

and highlands are generally comprised of glacial till. Soils formed from glacial till are typically

more impermeable than those formed from glacial outwash and alluvium. These glacial till soils

have a characteristic fragipan layer, which restricts infiltration into the deeper soil horizons and

may contribute to "flashier" stream responses to storm events (Gburek et. al 2006). Underlying

glacial soils is low permeability Devonian age mudstones and shale bedrock of the Upper Walton

formation (Horton et. al 2017). This material overlying the impermeable bedrock creates a

shallow unconfined aquifer system, typical in northern latitudes, that is highly sensitive to

surficial inputs and highly connected to surficial waters (Mullaney et. al 2009).
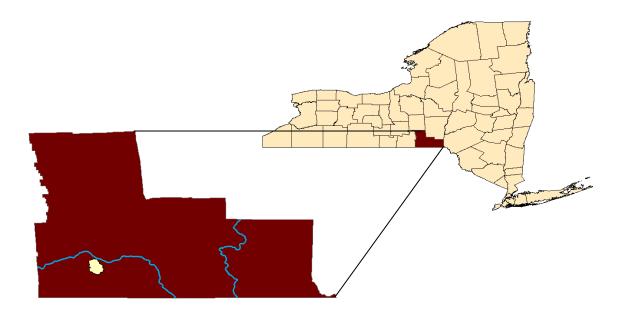
Figure 1.1.1- Location of the Fuller Hollow Creek Watershed within Broome County, NY. The
Susquehanna River is outlined within Broome County.

The scale of the Fuller Hollow Creek watershed makes it an ideal place to study urban

hydrology and geochemistry by eliminating the possibility for large scale geo-spatial and climatic

variations. The southern portion of the watershed is largely rural, with few residential areas, and

includes the Binghamton University Nature Preserve (Figure 1.2.2). This dramatically contrasts

with the northern portion of the watershed which is dominated by the Binghamton University

campus and surrounding suburban areas, where the majority of runoff from urbanized surfaces

intersects Fuller Hollow Creek at the confluence of three sub-watershed tributaries before

emptying into the Susquehanna River (Figure 1.2.2). The drastic variation in land use between

the upper and lower portions of the watershed provides an excellent opportunity to compare

the effects of urbanization with non-urban contaminant levels. Several groundwater wells that

penetrate both the surface glacial aquifer and deeper into the underlying shale bedrock aquifer

are situated in the northern half of the watershed enabling the study of contaminants in

groundwater as well as stream water to provide a more detailed assessment of the watershed.

1.1.2 Sub-watersheds

Fuller Hollow Creek is a 4.0 km long, Strahler classification 2nd order stream (Strahler,

1957). The lower 2.5 km of the creek have been artificially straightened and reinforced with

riprap to promote and protect local real estate. This is done at the expense of riparian

ecosystems, which are virtually non-existent for much of the streams length (Figure 1.1.2). The

Fuller Hollow Creek watershed can be divided into sub-watersheds which have varying land use

characteristics (Figure 1.1.3). Each sub-basin corresponds with a monitoring site of the same

name which are located at the terminus of each sub-watershed (Figure 1.1.4, Appendix A).
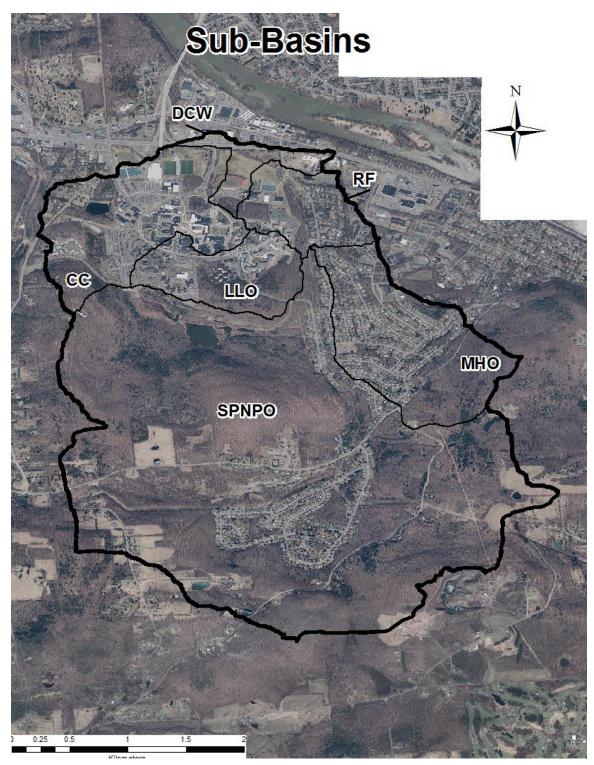
Figure 1.1.2- Sub-basins within the Fuller Hollow Creek Watershed. RF sub-basin includes inputs from SPNPO, MHO, and LLO. The DCW sub-basin includes inputs from SPNPO, MHO, LLO, CC, and RF. Aerial imagery courtesy of New York Sate GIS Clearinghouse, Broome County Ortho Imagery, 2014.

The SPNPO sub-watershed has the largest percentage of naturally forested area and lowest percentage of urban surface. This area encompasses the upper portion of the watershed and includes the Binghamton University Nature Preserve and rural and sub-urban areas. Fuller Hollow Creek flows through a small urban development and forested area in its upper portion which transitions into an artificially straightened stream channel for 63% of its length.

The MHO sub-basin encompasses a suburban area east of the Binghamton University campus. This area is drained by a small, 750m first order stream that intersects Fuller Hollow Creek just below the SPNPO sub-basin. Most of this stream channel is significantly altered and artificially reinforced to protect residential areas.

The LLO sub-basin is the smallest in area and has a very high urbanized percentage. Runoff from campus urban surfaces is directed into the Lake Lieberman retention pond before discharging into Fuller Hollow creek by way of a 160m 1st order stream.

The CC sub-basin has the highest urban percentage and drains the northwestern portions of the Binghamton University campus. Campus runoff is redirected through a series of culverts and storm drains that discharge into a roadside channel before entering Fuller Hollow Creek.

Land Cover
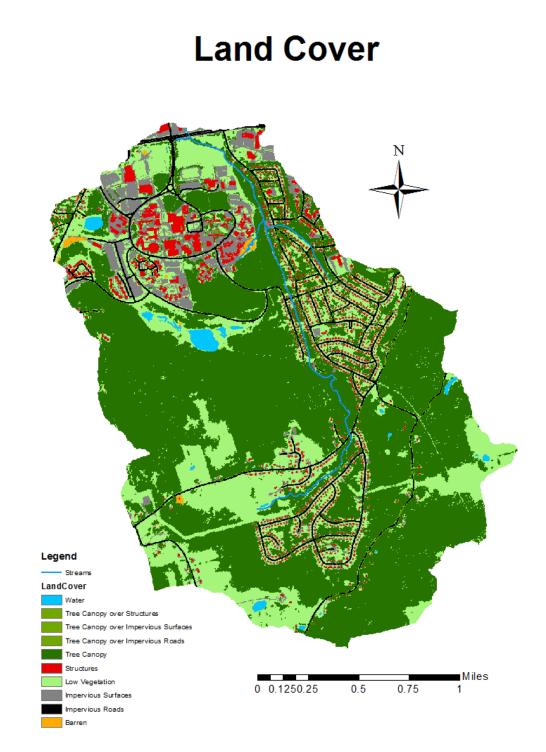
Figure 1.1.3- 2m landcover of the Fuller Hollow Creek watershed courtesy of Chesapeake Conservancy.
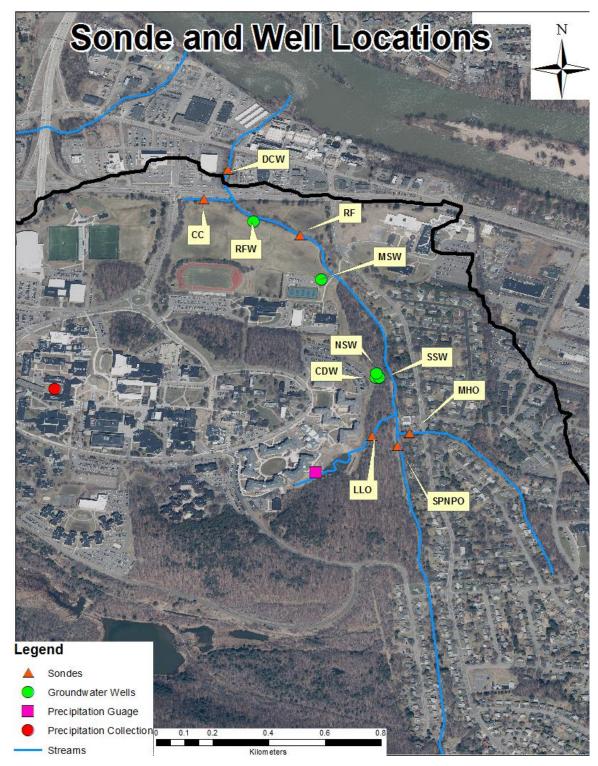
Figure 1.1.4- Stream sonde and groundwater well sites within the Fuller Hollow Creek Watershed (outlined in black). Aerial imagery courtesy of New York Sate GIS Clearinghouse, Broome County Ortho Imagery, 2014.

1.1.3 Groundwater Wells

The five monitoring wells sampled in this study are all located in the northern portions of the watershed between the buildings on the university campus and Fuller Hollow Creek (Figure 1.1.4, Appendix A). Of these five, four are positioned within the surficial alluvium and the remaining one within the shale bedrock. NSW and SSW sites are both 6.7m deep wells, that lie within the glacial till material on the east edge of the university campus, and are separated laterally by 20m. CDW is in the immediate vicinity of these wells but is open to the fractured shale bedrock aquifer at a depth of 37m. MSW is a 9.1m deep well that is positioned at the corner of a parking lot with casing recessed into the ground, but open to a surficial glacial outwash aquifer. RFW is a 12.2m deep well positioned just north of the university campus near Fuller Hollow Creek and is also open to the surficial glacial outwash aquifer.

1.2 Previous Work

The Fuller Hollow Creek Watershed (FHCW) has been host to several studies pertaining to both biologic and geological systems, conducted by Binghamton University researchers. Stream and groundwater sampling of the FHCW has been part of ongoing studies involving undergraduate and graduate education at Binghamton University for the last 10 years (Graney et. al 2008, Zhu et. al 2008). Specifically, students sample and lab test Fuller Hollow Creek and several groundwater wells at regular intervals throughout the Fall and Spring semester, additionally collecting streamflow and well head measurements. McCann (2013) was the first to use continuous recording of stage and conductivity from stream sondes to study the effects of retention pond structures, stream responses to storm events, and model contaminant transport through the FHCW by using the TR-20 model, with limited success. Johnson (2015) concluded

that continuous stream conductivity records from sondes could be used to accurately estimate chloride contaminant processes on nearby watersheds of comparable size and composition.

Evan and Davies (1998) assessed solute transport pathways within a watershed by means of Conductivity/Discharge (C/Q) hysteresis of storm events. Stream inputs may be modeled as a combination of surface runoff, soil water, and groundwater; which typically have varying solute concentrations which result in the formation of a hysteresis, or loop, when plotted against discharge over an event period. This model has been applied to a variety of watersheds in both salting and non-salting areas with varying results (Evans and Davies 1998, Rose 2003, Long et. al 2017).

Jin et. al (2011) refined and utilized the INCA-Cl model to quantify chloride levels within a larger eastern NY watershed, and subsequently simulated changes in stream chloride concentrations due to variable anthropogenic deposition. INCA-Cl is a dynamic mass balance model that simulates temporal variations of hydrologic flow within stream, soil water, and groundwater stores. Its proven success in modeling chloride values in a larger road salting impacted watershed make it an ideal choice for simulating responses in the small, multi-land use Fuller Hollow Creek Watershed.

1.3 Hypothesis

This study aims to achieve the following goals; (1) determine what impact impervious surfaces and road salting have on long-term stream and groundwater chloride concentrations. (2) Determine how road salts disperse through watersheds and identify areas of pollutant storage. Determine if a C/Q hysteresis model can identify variable pollutant contributions from groundwater, soil water, and surface runoff in an urban environment. (3) Determine if the

INCA-Cl model can accurately quantify stream chloride concentrations in a small urban watershed and predict chloride levels under alternative depositional scenarios.

Based upon the characteristics of the Fuller Hollow Creek watershed and sub-watersheds, the following hypothesis are proposed:

1. Total dissolved ions in stream and groundwater will increase over time with rates higher in more urbanized sub-watersheds than less urban ones. All major cations within both stream and groundwater are expected to increase in concentration over the study period, with sodium having the most dramatic increase.

2. Several reservoirs of pollutant storage will be identified of varying contribution to stream conductivity based upon season and landuse as well as hysteresis loop analysis. Surface runoff will be the dominant chloride contributor during the salting season (December-March), while groundwater will be the dominant contributor in the non-salting season (April-November).

3. INCA-Cl will be able to reasonably simulate chloride values within Fuller Hollow Creek but may fail to predict behavior in the more complex sub-watersheds. Variable chloride deposition scenarios will have a moderate impact on the model output.

The results of this study may be used to better understand how road salting practices impact urban watersheds by assessing how road salts disperse after deposition. By quantifying the effects of these practices through the utilization of a readily applied model, one can determine the minimum amount of change in chloride loading necessary to make a significant impact on threatened urban ecosystems, which is applicable to many areas. As far as we know this is the first study to couple the use of geochemistry with hysteresis curves and the INCA-Cl

model to document long term surface and groundwater chloride storage and movement within

a multi-landuse watershed.

Chapter 2 Methods

2.1 Road Salt Contamination Proxies

Electrical conductivity is the measurement of the electrical current passing through a

solution, with units of micro Siemens per centimeter ($\mu S\ cm^{-1}$). This measurement is dependent

on the type and concentration of ions in a solution and temperature of the solution; therefore, it

is necessary to normalize all specific conductivity measurements to a standardized 25°C.

Conductivity may be used as a proxy for total dissolved solids (TDS) of a solution by multiplying

by a constant. This paper will use the commonly used freshwater scale factor to estimate the

TDS of solution (Eq. 2.1)

Eq. 2.1

$$TDS= SC* 0.7$$

TDS = Total dissolved solids (mg/L)
SC = Specific Conductance (µS/cm)
0.7= Freshwater scaling factor

2.2 Historical Data

Data from Binghamton University undergraduate field studies over a 10-year period (fall

2006-spring 2016) provided an excellent source of information for a long-term study of stream

and groundwater geochemistry within the Fuller Hollow Creek watershed. To determine if the

Fuller Hollow Creek watershed is subjected to accumulation of NaCl contamination, and the

degree of its effects, existing archives of long-term stream and groundwater cation and TDS

concentration data within the watershed were evaluated.

In the archived datasets, stream and groundwater samples were collected regularly at 1-

week intervals during the spring and fall semesters (6-12 weeks total), along with streamflow

and ground water head measurements (with the exception of groundwater data for fall 06, 07,

and 08). Groundwater and stream total dissolved solids (TDS) were measured from in-lab

electrical conductivity probe measurements. Cation concentrations were determined by direct

current plasma spectroscopy (DCP) prior to fall 2011. After 2012 period ion concentrations were

determined by inductively coupled plasma optical emission spectrometry (ICP-OES). Of the

cations measured, Na, Ca, Mg, and K were analyzed in this study.

SPNPO sites were only sampled in the spring, however, its sub-basin components (SP

and NPO) were sampled in the fall. Concentrations of TDS and cations for SPNPO were obtained

using discharge measurements from the SP and NPO sites to approximate the SPNPO site values

(Eq. 2.2).

Eq. 2.2

$$(Q_{SP} \times C_{SP}) + (Q_{NPO} \times C_{NPO}) = (Q_{SPNPO} \times C_{SPNPO})$$

$$((Q_{SP} \times C_{SP}) + (Q_{NPO} \times C_{NPO})) / Q_{SPNPO} = C_{SPNPO}$$

Q = Discharge (l/s)
C = Solute Concentration (mg/L)
SP = Stair Park sub-basin
NPO = Nature Preserve sub-basin
SPNPO = Combined Stair Park and Nature Preserve sub-basins

The archived data used in this study consists of median values from each sampling

season. Median values were used rather than season averages because of the small sample size

(6-12/ site/ season) and because any significantly large storm event during the time of collection

may provide a low seasonal average for TDS measurements. Standardizing TDS concentrations with streamflow is challenging over this long-term study due to some inconsistencies in measurement technique, equipment, and unrecorded data. The geochemistry and hydrology of Fuller Hollow Creek varies drastically by season; therefore, analysis of historical data is presented both separately by season as well as holistically to more accurately identify trends within the data.

2.3 Sonde Deployment

To better understand how road salts disperse through watersheds, a stream sonde network was deployed to obtain high frequency geo-chemical and physical data over a one-year period. These devices gathered data on stream conductivity, temperature, and stream stage in 15-minute intervals at 6 locations corresponding with each sub-watershed and the outlet of the Fuller Hollow Creek watershed (Figure 1.2.4, Appendix B). These measurements were recorded using Hydromet® OTT sondes to provide a continuous 12-month dataset for each site (Figure 2.3.1). A sonde was positioned in the FHC prior to any culverted inflows to the stream at site SPNPO, thus representing less urbanized conditions (Figure 1.2.4). Three sondes were placed at major inflows of urban runoff to the FHC (sites MHO, LLO, CC). The remaining two sondes (sites DCW and RF) were placed in the main channel, one near the terminus of the watershed and the other in the lower channel.

Figure 2.3.1- Recording interval for all deployed sondes. Several hour to day long gaps exist in the DCW recording data. RF data was only acquired towards the end of the study period.

2.3.1 Water Sampling

Grab samples of stream water corresponding to each sonde location were collected on a weekly basis over the study period of June 2015 – June 2016. These samples were lab tested for electrical conductivity, anions and major cations. Groundwater samples were collected at five well locations on the Binghamton University campus near Fuller Hollow Creek (Figure 1.2.4). Groundwater head, temperature, and grab samples from each of the wells were collected every 1-2 weeks. Samples were lab tested for electrical conductivity, anions, and major cations in the same manner as stream samples.

2.3.2 Sonde Calibration

Prior to installation, each sonde was calibrated for temperature and conductivity with the provided software and a 500µS/cm conductivity standard. Weekly stream grab samples,

corresponding with each sonde site, were lab tested for conductivity by an Omega® CDH-42

conductivity probe. Sonde conductivity values were recorded at each grab sample interval and

compared to calibrate conductivity at a range of values throughout the duration of their

deployment (Appendix D).

Stream discharge was measured weekly to estimate discharge at each sonde location

(Eq. 2.3.1). Under variable flow conditions, measurements were conducted using a Swoffer®

model 2100 velocity meter in accordance with USGS standards (Rantz et al, 1982).

Eq. 2.3.1

$$Q = (W_1 D_1 v_1 + W_2 D_2 v_2 ... + W_n D_n v_n)$$

Q = Discharge (m^3/s)
W = Width of stream sub-section (m)
D = Depth at the center of the stream sub-section (m)
v = Average water velocity at 0.6 of the water depth (m/s)
n = Number of measurement points

A rating curve was generated for each sonde relating recorded stage with measured

discharge at each site (Appendix C). At the DCW and RF sites multiple rating curves were used

due to dislodgment and subsequent repositioning of stream sondes during storm events. A pre-

existing weir was used for determination of discharge at the CC site. McCann (2012) determined

the optimal equation for the CC site weir (Eq. 2.3.2).

Eq. 2.3.2

$$Q= K (L - 0.2H) H^{1.5}$$

Q = Discharge (l/s)
L = Width of the weir (m)
H = Height of the water over the sub-section being measured
K = Constant determined by weir type and output units, equal to 1838 (for L/s)

Low baseflow conditions and the flashy nature of Fuller Hollow Creek made it difficult to conduct discharge measurements during high flow, this is especially true of the MHO site. Due to these circumstances high flow is not calibrated with the same accuracy as low flow conditions, and in some instances discharge values were determined by extrapolating beyond the calibrated range of the rating curve.

2.3.3 Dissolved Ion Calibration

Continuous conductivity data from stream sondes was used as a proxy for dissolved ions within solution. Concentrations of Cl anions as well as common cations Na, Ca, Mg, and K from weekly grab-samples were calibrated with their corresponding conductivity values with an empirical linear regression (Eq. 2.3.3, Appendix D).

Eq. 2.3.3

$$C_{ion}=SC(\mu S/cm)*\beta$$

C_{ion}= ion concentration (mg/L)
SC= Specific Conductivity (μS cm^{-1})
β= Conversion factor

Dissolved Ion Increase (mg/L) per Increase in Conductivity (uS/cm)			
	Chloride	Sodium	Calcium
DCW	0.280	0.142	0.071
RF	0.370	0.114	0.069
SPNPO	0.181	0.087	0.111
MHO	0.310	0.131	0.051
LLO	0.293	0.163	0.046
CC	0.297	0.208	0.028

Table 2.3- Calibration slopes of dissolved ion concentrations relative to sonde conductivity at each site. (Appendix D)

2.3.4 Precipitation

Precipitation measurements were continuously collected by an Onset® tipping-bucket rain guage positioned within the watershed (Figure 1.2.4). Due to the small size of the watershed a single site was deemed sufficient for estimated precipitation over the study area. In addition, a single precipitation collector was used to capture rainfall to measure precipitation conductivity and dissolved ions (Figure 1.1.4).

2.4 Pollutant Retention

Total sodium and chloride loads were calculated for each site on a daily basis to better understand retention of these two components within the watershed (eq. 2.4.1). Sodium and chloride concentrations of stream loads were determined through calibrated sonde conductivity data (Appendix D).

Eq. 2.4.1

Na load (kg/day) = (Na$^+$ (mg/L) x 1kg/1000000mg) x (Q(m^3/s) x 1000L/m^3) x 900s/day
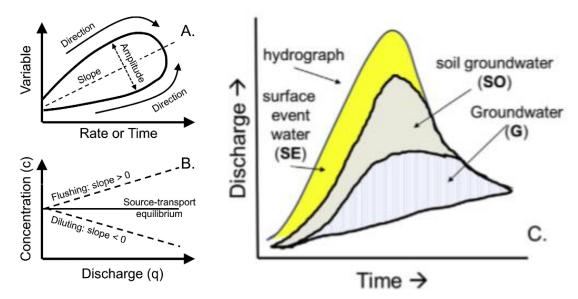
Cl load (kg/day) = (Cl$^-$ (mg/L) x 1kg/1000000mg) x (Q(m^3/s) x 1000L/m^3) x 900s/day

Na$^+$ = Calibrated sodium concentration from sondes
Cl$^-$ = Calibrated chloride concentration from sondes
Q = Discharge
s= Seconds

Calculated loads were compared to atmospheric and road application deposition estimates to give the percentage of each ion retained within soil and groundwater. Differences in sodium and chloride loads can be used to identify NaCl saturation state within soil reservoirs and estimate cation exchange within the Fuller Hollow Creek watershed.

2.5 C/Q Hysteresis, Identifying Pollutant Concentration Sources

Conductivity/Discharge (C/Q) hysteresis of storm events provide a method for assessing solute transport pathways within a watershed. For a given storm event, stream inputs may be modeled as a combination of surface runoff (SE), soil water (SO), and groundwater (G) inputs (Figure 2.5.1c). These three water components typically have varying solute concentrations which result in dynamic chemical fluctuations over storm event periods. Solute concentrations plotted against discharge over an event period form a hysteresis, or loop (Evans and Davies 1998). Variations in loop direction, curvature, and slope determine the relative importance of each input constituent.

Figures 2.5.1-(*a*) Figure detailing C/Q parameters of rotational direction, slope, and amplitude (curvature). (b) Figure illustrating the association between slope and flushing/dilution. (c) Figure depicting the modeled 3-component hydrograph for use in the C/Q hysteresis model (Evans and Davies 1998).

Rotational direction is influenced by the timing of the discharge peak relative to the concentration peak (figure 2.5.1a). If the concentration peak occurs before the discharge peak

(C_{SE}>C_{SO}), then the rotation will be clockwise. Conversely, If the concentration peak occurs after the discharge peak (C_{SE}<C_{SO}), then the rotation will be anti-clockwise (Evans and Davies 1998).

The curvature of the hysteresis loop is mostly influenced by the groundwater concentration. If groundwater concentration is intermediate relative to the other components the loop will be completely convex. If groundwater is higher or lower than surface and soil water than one limb of the loop will be concave (Evans and Davies 1998).

The slope of the C/Q plot is indicative of flushing high concentration water over the course of an event or dilution from high discharge surface and soil water. The general trend or slope of a concave system will determine whether groundwater has the highest or lowest concentration. A positive slope indicates high conductivity surface flow from a flushing event whereas a negative slope indicates higher concentrations in baseflow (Evans and Davies 1998, Long et al 2017).
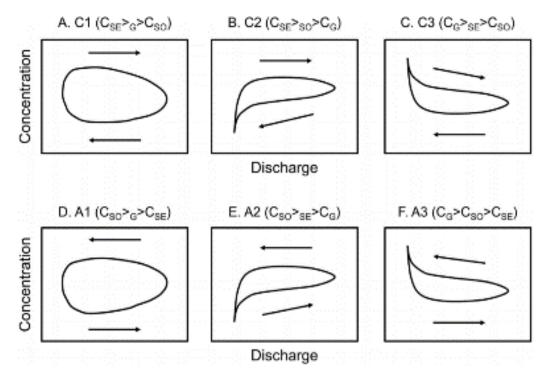
Figure 2.5.2- The six classifications of C/Q hysteresis curves with accompanying interpretations (Evans and Davies 1998)

Chloride values within most watersheds are primarily controlled by the mixing of low

chloride surface water from storm events and higher concentration groundwater. This pattern

becomes inverted during the winter months when urban surfaces contribute salt loads resulting

in high surface and groundwater concentrations. Considering the dominant source of these ions

are derived from road salt application, an Evans-Davies C1 or C2 type behavior is expected to be

observed due to flushing from urban surfaces during the salting season. It is also expected that a

variation from this trend may be observed at the LLO site, in which A1 type behavior would be

most characteristic of a retention pond outlet that mitigates pollutant concentration and large

fluctuations in discharge. Pollutant storage and subsequent concentration in groundwater

during summer and fall months will likely produce C3 or A3 type curves with groundwater being

the highest concentration source.

2.5.1 Storm Selection

Storm events of various intensity and time of year were examined to determine the

amount of variability in concentrations present within the watershed. Six storm events were

subsequently selected for Conductivity/Discharge (C/Q) Analysis. Half of the events selected

were chosen within the salting season (December-March), while the other half were within the

non-salting season (April-November). Selecting events from throughout the one-year study

period allows for the analysis of changes that may occur in differing areas of pollutant

contribution. Hysteresis curves from each event were produced for each sonde site to

determine how spatial variations affect changes in component concentration throughout the

watershed. The interpretations of each hysteresis loop are based upon the assumption that

each event has a relatively constant precipitation rate throughout the event duration, as

changes in precipitation rate may add additional hysteresis curves or lead to wrong

interpretations due to deviations from a normal hydrograph; therefore, only events that met these criteria were analyzed.

Conductivity was selected as the modeled component to be plotted against discharge due to the high frequency data from stream sondes and all elemental concentrations having a linear correlation with observed conductivity. Based on prior studies Na^+ and Cl^- are the primary dissolved ions within the watershed, and thus the primary contributors to stream conductivity.

2.6 INCA-Cl Model Setup

Inputs to the INCA model include geospatial data from a GIS interface, estimation of chloride inputs to the watershed based upon land cover and chloride loading, and weather data for daily moisture balances. The Fuller Hollow Creek watershed was divided into five sub-basins corresponding with each sonde site; an upstream basin (SPNPO), a midstream basin (RF), three basins corresponding with major urban tributaries (MHO, LLO, CC), and the overall watershed (DCW). Sub-basin dimensions were determined using ArcGIS® basin delineation tool with a 2m digital elevation model (NYSGIS Portal). National land cover data (NLCD 2011) was used to determine land cover within the entire watershed and each sub-basin. The 13 classifications present in the watershed were combined into four, those being forest, short vegetation (grass and shrub), arable (agriculture), and urban (Figure 2.6.1a-b).

NLCD 2011 Land Cover Classification	INCA-Cl Land Cover Classification
Deciduous Forest	
Evergreen Forest	Forested
Mixed Forest	
Woody Wetlands	
Grassland/Herbaceous	
Shrub/Scrub	Short Vegetation
Developed, Open Space	
Emergent Herbaceous Wetlands	
Pasture/Hay	Arable
Cultivated Crops	
Developed, Low Intensity	
Developed, Medium Intensity	Urban
Developed High Intensity	

Figure 2.6.1a- Combined NLCD land cover classification for input to the INCA-Cl model.

INCA-Cl Land Cover Fuller Hollow Creek Watershed

Urban 21%

Arable 4%

Short Vegetation 15%

Forested 60%

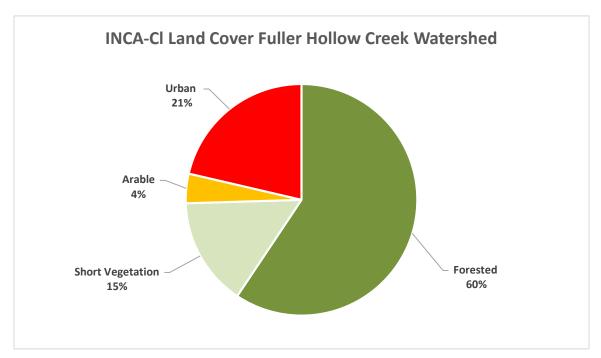Figure 2.6.1b- Fuller Hollow Creek Watershed land cover from 2011 NLCD dataset reduced to four INCA-Cl land cover inputs.

Estimation of chloride input to the Fuller Hollow Creek watershed was constrained to three major sources; road salt application to campus roadways and parking lots, as well as town roadways, and atmospheric deposition. Road length within the watershed, necessary for salting

25

estimations, was determined through ArcGIS®. There is a total of 22.5km of lane roadways on

Binghamton University campus with 55.4km of municipal lane roadways in the surrounding

area. The Binghamton University campus uses approximately 1085 metric tons/ year of NaCl on

road surfaces, this equates to 48.35 metric tons NaCl/ lane km per year (Donald Williams,

Binghamton University Physical Facilities, personal communication). Deposition to town roads

was based upon NYS DOT estimates of an average application rate of NaCl for residential roads

at approximately 9.36 metric tons NaCl/ lane km per year (National Research Council, 1991);

totaling 518.8 metric tons of NaCl per year deposited within the FHC watershed. Atmospheric

wet chloride deposition within the FHC watershed was estimated to be 0.997 kg/ha/year

totaling just 1.6 metric tons/ year (National Atmospheric Deposition Program). The total annual

NaCl deposition to the FHC watershed is estimated at 1606 metric tons/ year, 67.6% from

campus roadways, 32.3% from town roadways, and 0.1% atmospheric.

The INCA-Cl model calculates stream discharge by estimating daily hydrologically

effective rainfall (HER), and soil moisture deficits (SMD). Hydrologically effective rainfall can be

defined as "the amount of precipitation that penetrates the soil surface after allowing for

interception and evapotranspiration losses" (whitehead 1998a). Soil moisture deficit estimates

were derived from the calculated actual evapotranspiration (AET) and precipitation. Soil

moisture was assumed to be zero for the initial starting conditions on January 1, 2015 (Eq. 2.6.1,

Appendix E). This results in an initial SMD and HER value of zero, as it is reasonable to assume

these values for winter in upper New York State (Limbrick, 2002). AET was determined by

applying a root constant to the potential evapotranspiration (PET) calculated with the United

Nations Food and Agriculture Organization Pennman-Monteith Soil Moisture Model (Eq. 2.6.2).

Model inputs include daily mean, maximum, and minimum temperature, minimum and

maximum air pressure and humidity, as well as mean dew point temperature. Estimated values

for wind speed, vapor pressure, and net solar radiation were estimated rather than directly measured; wind speed was assigned a constant of 2 m/s, with radiation being function of latitude (Allen et. Al 1998).

Eq. 2.6.1

Soil Moisture Deficit (SMD):

$SMD_i = SMD_{i-1} - P_i + AET_i$ $SMD_{i-1} > P_i - AET_i$

$SMD_n = 0$ $SMD_{i-1} < P_i - AET_i$

Hydrologically Effective Rainfall (HER):

$HER_i = P_i - AET_i - SMD_i$ $SMD_i < P_i - AET_i$

$HER_n = 0$ $SMD_i > P_i - AET_i$

Actual Evapotranspiration (AET) Root Constant Thresholds:

<74mm = 100% PET

>75mm = 65% PET

>100mm = 45% PET

Eq. 2.6.2

$$ET_o = \frac{0.408\Delta(R_n - G) + \gamma \frac{900}{T+273} u_2 (e_s - e_a)}{\Delta + \gamma(1 + 0.34u_2)} \quad (6)$$

where

ET_o reference evapotranspiration [mm day^{-1}],
R_n net radiation at the crop surface [MJ m^{-2} day^{-1}],
G soil heat flux density [MJ m^{-2} day^{-1}],
T mean daily air temperature at 2 m height [°C],
u_2 wind speed at 2 m height [m s^{-1}],
e_s saturation vapour pressure [kPa],
e_a actual vapour pressure [kPa],
$e_s - e_a$ saturation vapour pressure deficit [kPa],
Δ slope vapour pressure curve [kPa °C^{-1}],
γ psychrometric constant [kPa °C^{-1}].

2.6.1 Model Input and Calibration

Calculated discharge and chloride concentration values obtained from stream sonde data, corresponding with the terminus of each sub-basin, provides a method for calibrating model parameters. Calculated discharge from an empirically generated rating curve at each sonde site was used to calibrate discharge within the INCA model by adjusting groundwater and soil water velocity and retention time parameters (Appendix E). Chloride concentrations from campus groundwater wells were used to approximate initial concentrations within the modeled variable soil and groundwater land cover reservoirs. Chloride levels from calibrated sonde conductivity, validated by ion chromatography of weekly grab samples, were compared to INCA-Cl estimates to ensure accurate results.

The model parameters were calibrated to the DCW, RF, and SPNPO sites before being applied to the remainder of the watershed. The main stream sites were first calibrated because each tributary has its own unique influences (storm sewers at CC, and retention pond at LLO) that are not applicable to the watershed as a whole. Calibrating INCA to a larger, more "normal" stream allowed for an easier understanding of how each model component influenced outputs which could then be adjusted for each tributary independently. INCA-Cl was modeled for a 535-day period from January 1st, 2015 through June 18th, 2016 to encompass the entire study period.
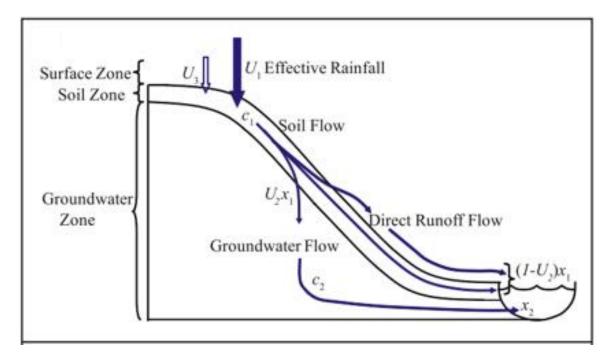
Figure 2.6.2- Illustration of the INCA-Cl catchment model component distribution (from Jin et. al 2011). See Appendix E for model equations.

Chapter 3 Results and Discussion

3.1.1 Long-Term Study, Fall Data

Median fall stream TDS, cation, and anion concentrations represent baseflow conditions within Fuller Hollow Creek. A large soil moisture deficit, persistent throughout late summer and throughout autumn, is typical in upstate NY (figure 3.1.1). Water within Fuller Hollow Creek during this season is largely confined to pools within its upper portions and average discharge is typically under 50 L/s in the lower portions.
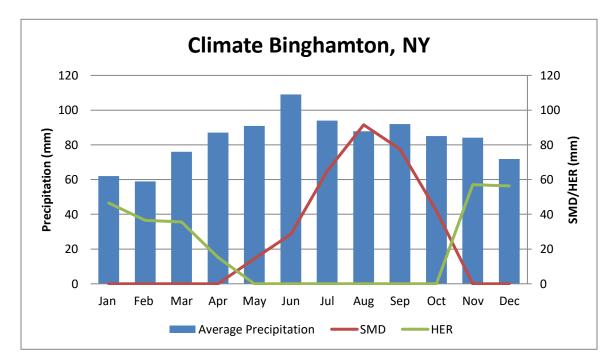
Figure 3.1.1- Climate data from Greater Binghamton Airport 1960-2000. SMD represents monthly average soil moisture deficits. HER represents monthly average hydrologically effective rainfall. These conditions represent baseflow from May through November observed in Fuller Hollow Creek.

All sampled sub-basins show a slightly increasing trend in TDS over the 10-year interval (Figure 3.1.2). Based on the slope of the linear trends, the MHO site showed the least amount of increase of 11.5mg/L per year. CC and LLO sites have the largest increase of 31.8mg/L and 34.7mg/L per year respectively. Of the two main channel stream sites sampled, the SPNPO site, which has roughly 3% impervious surface, experiences an increase of 14.1mg/L/year while the downstream RF site showed an increase of 26.2 mg/L/year. Fall of 2011 experienced record high rainfall of over twice the seasonal average. This corresponds with a minimum all stream TDS values for all sites (except CC) due to dilution of stream waters from precipitation.
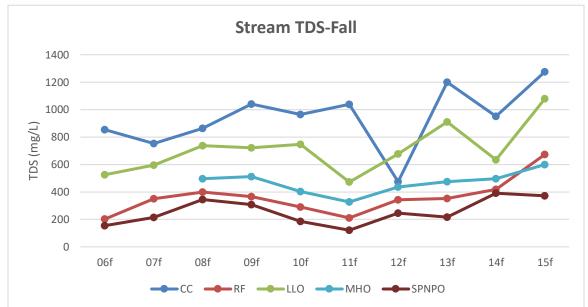
Figure 3.1.2- Stream fall median TDS values from archived and acquired data.

Stream TDS Increase/ Year- Fall	
Site	TDS Increase (mg/L/year)
CC	31.84
LLO	34.67
MHO	11.49
RF	26.19
SPNPO	14.03

Table 3.1.1- Fall stream TDS increase/year determined by linear regression.

Calcium values are highest at the CC and LLO sites but have no significant trend over the study period. The SPNPO, RF, and MHO sites all have a general increase in calcium between 2 and 4mg/L/year. All sites show a general increasing trend with respect to sodium over the last 5 years. Sodium also is the most abundant major element analyzed. CC, LLO, and RF sites all experience an average increase in sodium of approximately 20mg/L/year whereas MHO and SPNO experience a 5 and 10mg/L/year increase respectively.

3.1.2 Long-Term Study, Spring Data

Streamflow within Fuller Hollow Creek in the spring is significantly higher than the fall; with an average downstream baseflow discharge typically exceeding 170 L/s. Snowmelt and decreased evapotranspiration are the primary source of groundwater recharge and subsequent increased baseflow over this interval.

As with fall values, all stream sites experience an increase in TDS over the study period (Figure 3.1.3). CC and LLO sites have elevated TDS values compared to their fall values and the other sampling sites. Increasing TDS trends range from as high as 146.4mg/L/year at the CC site to just 3.8/year at the SPNPO site.
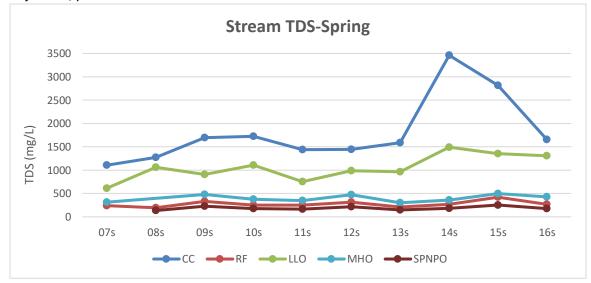
Figure 3.1.3- Stream spring median TDS values from archived and acquired data.

Stream TDS Increase/ Year- Spring	
Site	TDS Increase (mg/L/year)
CC	146.42
LLO	66.56
MHO	7.58
RF	8.89
SPNPO	3.83

Table 3.1.2- Spring stream TDS increase/year determined by linear regression.

Calcium concentrations in the spring show a slightly increasing trend at all sites while magnesium values stay generally constant throughout the study period. All sites show a definitive increasing trend in Sodium over the 5-year period. Tributaries CC, LLO, and MHO have a higher rate of sodium increase in the spring while the opposite is true of the main channel RF and SPNPO sites.

3.1.3 Discussion of Overall Trends in Streams

TDS concentrations within Fuller Hollow Creek appear to be increasing at all the sites sampled over the duration of the sonde deployment with higher variability in sub-watersheds with higher TDS concentrations (Figure 3.1.4). The two sub-basins with the highest impervious surface (CC and LLO) consistently have the highest concentrations of all four major cations; however, they tend to have a negative trend with regards to Ca in the fall and K in the fall and spring. Calcium values are also significantly lower in the fall and higher in the spring at these two sites (Appendix F).
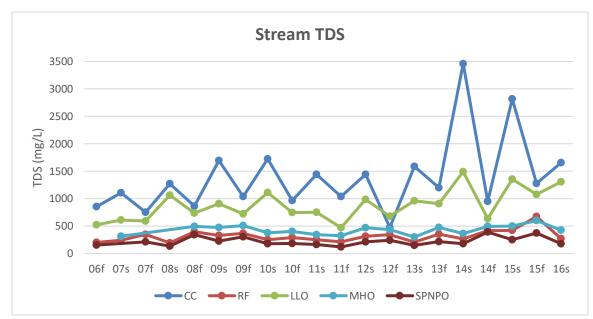
Figure 3.1.4- Stream median TDS values from archived and acquired data.

Stream TDS Increase/ Year	
Site	TDS Increase (mg/L/year)
CC	50.84
LLO	27.71
MHO	4.68
RF	8.06
SPNPO	3.62

Table 3.1.3- Stream TDS increase/ year determined by linear regression.

The Binghamton University campus applies approximately 16.3 metric tons of calcium-magnesium acetate ($CaMg_2(CH_3COO)_6$) to walkways during winter months as an alternative de-icing agent to NaCl (in contrast to the 1607 metric tons of NaCl applied to roadways). This was considered when identifying the source of elevated calcium levels, however, magnesium concentrations do not exhibit the same behavior as calcium despite being applied in similar concentrations in this deicer. Therefore, calcium magnesium acetate was not considered to be a significant contributor to calcium concentrations within the Fuller Hollow Creek watershed. The source of the anomalously high calcium concentrations during the spring likely involves processes in the urban runoff dominated systems at these two sites. The large amounts of NaCl

applied during the winter months will leach calcium from concrete surfaces at an accelerated

rate, thus resulting in elevated dissolved calcium in these reaches in the spring (Wan et al 2005,

Kaushal et. al 2017).

The LLO and CC site show much more variability in TDS concentrations than other sites

with lesser TDS levels. Similar trends were observed by Kelly et al. 2008 and Daley et al. 2009 in

multi-decade studies on northeastern streams. In both studies, concentrations increase steadily

until reaching a threshold level, then greatly fluctuate while maintaining a slightly increasing

trend. The trends in sub-basins with high TDS values within Fuller Hollow Creek appear similar to

these large-scale fluctuations observed in these studies. Analysis of sodium and chloride

retention is needed to determine the extent of road salt saturation in shallow aquifers and

potential differences in saturation between the sub-watersheds.

Urban hydrology also influences the sodium and overall TDS values when comparing

tributaries and the main stream. The RF and SPNPO sites consistently experience lower sodium

and TDS values in the spring whereas CC and LLO have lower values in the fall. Bypassing natural

systems of infiltration, water in these more urbanized systems at CC and LLLO flows directly to

streams thus increasing sodium and TDS values during salting seasons.

3.1.4 Correlation with Impervious Surface

TDS values in streams over the course of the study have a positive correlation with the

percent imperviousness of their corresponding sub-basin, which is consistent with a watershed

where the primary pollutant is road salt. Figure 3.1.5 relates the imperviousness of each sub-

basin with the averaged median seasonal TDS values over the study period. Results are similar

to findings in Daley et al. (2009) and Heisig (2000), which have Na and Cl concentrations in

baseflow with impervious surface in several northeastern streams over several

decades. This study finds Na and Cl to have a direct relationship with the percent of

impervious surface in the sub-basins of the Fuller Hollow Creek watershed.

TDS vs Impervious Surface

$y = 32.822x + 49.607$
$R^2 = 0.886$
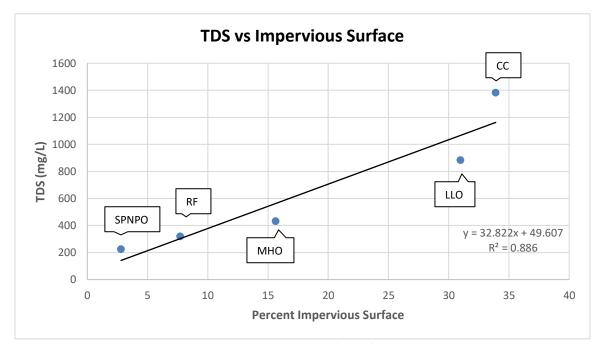
Figure 3.1.5- Plot relating the percent impervious surface of each sub-watershed with the average median stream total dissolved solids over the 10-year study period.

The two sites that fall below the best fit linear regression are MHO and LLO, these

discrepancies can be explained by the variation in road salt inputs and hydrology at these sites.

The MHO site drains a suburban area adjacent to the university campus; the road salt

application rate for these roads is estimated to be only 20% per lane mile of the amount applied

to campus roads that contribute to the RF, LLO, and CC sites. The LLO site may be lower than

expected due to the retention pond immediately upstream of the sample site. McCann (2013)

showed that retention pond structures, and specifically the Lake Lieberman pond, will mitigate

TDS levels entering Fuller Hollow Creek due to groundwater contributions. Concentrations of

major cations Na, Ca, Mg, and K also strongly correlate with percent imperviousness of each

sub-basin (Appendix G). This lends support to the hypothesized cation exchange occurring in

soils and urban surfaces due to a large influx of sodium as discussed later.

Changes in impervious surface were also considered over the study interval to be a potential source for the increasing TDS values over the study period as an alternative to the pollutant retention in soil and groundwater hypothesis. Beginning in spring of 2008, the Binghamton University campus constructed several large on-campus housing structures adding to the imperious surface of the FHC watershed and greatly affecting drainage to Fuller Hollow Creek from the LLO site (Appendix A). This building project expanded the Lake Lieberman retention pond structure, which captures runoff from a significant portion of the impervious surfaces on campus. The average rate of TDS increase per year over the study period was plotted against the amount of increase in impervious surface to determine any significant relationships (Figure 3.1.6). Despite no change in imperviousness in the SPNPO sub-basin, and a less than 1% increase in the MHO sub-basin, TDS rates still increase. This indicates that a change in impervious surface alone cannot account for an increasing trend in TDS. Furthermore, the CC site experiences a much larger rate of TDS increase than the LLO and RF sites despite a smaller increase in impervious surface percentage (Table 3.1.4).

Impervious Surface Percentages of FHC Sub-basins			
	2006	2011	% Increase
DCW	10.62	11.15	5.04
RF	7.31	7.7	5.42
SPNPO	2.8	2.8	0
MHO	15.51	15.62	0.72
LLO	27.72	30.97	11.72
CC	32.34	33.9	4.83

Table 3.1.4- Table of impervious surface change in the Fuller Hollow Creek watershed.

TDS Increase vs Impervious Surface Increase

$R^2 = 0.2405$
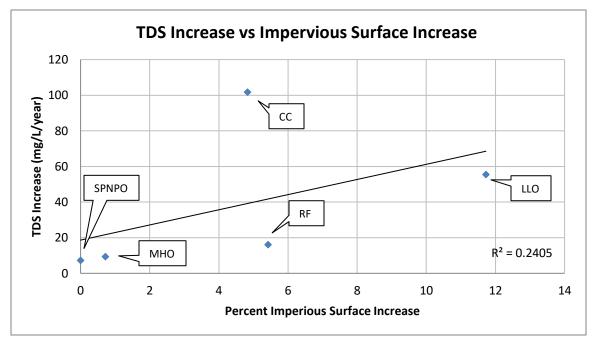
Figure 3.1.6- Plot relating the increase in percentage of impervious surface of each sub-watershed with the increase in average median stream total dissolved solids per year over the 10-year study period.

3.1.5 Groundwater Analysis

Samples from MSW and CDW show little to no net increase in TDS over the past 10 years, however, the CDW site experiences an interval of elevated TDS from spring of 2010 through spring of 2012 (Figure 3.1.7). MSW also experiences an anomalous peak in spring of 2011. These intermittent periods of elevated TDS are not shared by the NSW or SSW sites. A potential explanation for the elevated TDS levels at the CDW site may be the expansion of university housing in the well site's vicinity, which began in fall of 08 and was completed in spring of 13.
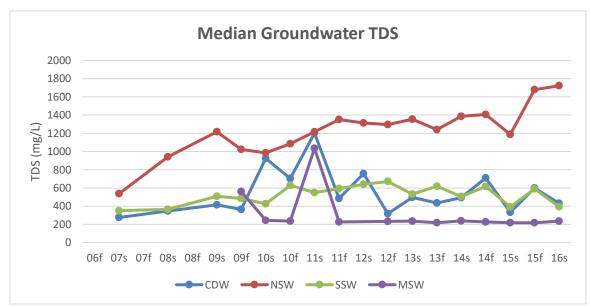
Figure 3.1.7- Groundwater median TDS values from archived and acquired data.

Groundwater TDS Rate of Increase	
Site	TDS Increase (mg/L/year)
CDW	3.8
NSW	88.8
SSW	11.7

Table 3.1.5- Groundwater TDS increase/ year determined by linear regression.

Samples from SSW and NSW have an increase in TDS of 11.7mg/L/year and 88.8mg/L/year over the study interval (Appendix F). The NSW site also has TDS concentrations that are consistently over twice as high as the SSW site, despite being separated laterally by 20m and drilled to the same depth within the surficial aquifer. The NSW well also has the highest vales of Ca, Mg, and Na and the only consistent increase of these cations over the study period. This includes an increase of 10.2mg/L/year and 2.2mg/L/year for Ca and Mg, and a 4.0mg/L/year increase in Na over the last five years.

Preferential flow paths within the glacial till sediment provide an explanation for the discrepancy between these two sites. A study by Bianchi et al. 2011 demonstrates how the 5% fastest flow paths within a shallow heterogeneous aquifer can account for 40% of groundwater flow. A similar situation of high permeability sub-surface lenses within the Fuller Hollow Creek watershed could account for elevated contaminant levels in the NSW well by providing a conduit for contaminated infiltration from urban sources. Contaminated groundwater sourced from urban runoff would follow paths of low permeability thus reducing mixing with uncontaminated groundwater. These hypothesized preferential flow paths may either be the result of natural glacial deposits or alternatively "urban karst" (Perera et. al 2013). The term urban karst is used to distinguish urban sub-surface features, such as artificial fill or electrical conduit pathways that can potentially affect groundwater flow within shallow aquifers.

The primary cations observed within groundwater are calcium and sodium, both occurring in similar concentrations. Of the major cations, calcium is the only one to consistently fluctuate by season over the study period, with concentrations elevated in the spring months relative to the fall for all sample sites (Appendix F). One potential mechanism for this drastic fluctuation of calcium could be cation exchange within soils (as discussed later). This would provide an explanation for the elevated levels during the spring, during and immediately following the salting season.

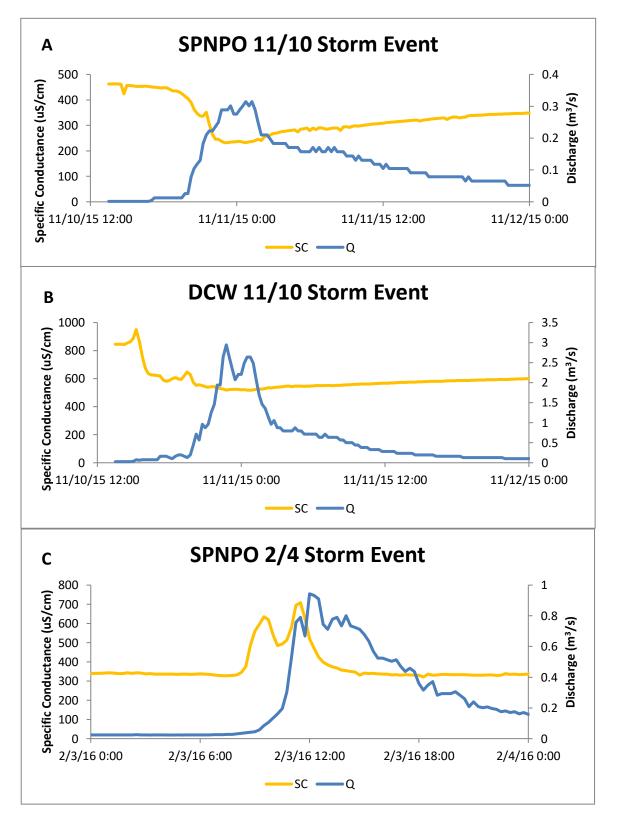**3.2 Real-Time Stream Data, Seasonal Variations**

Sonde generated data at each site is divided into hydrologic season; summer (June, July, August), fall (September, October, November), winter (December, January, February), and spring (March, April, and May) to identify characteristics in hydrology and stream chemistry associated with each period. Summer conditions in the Fuller Hollow Creek are characterized by

low flow (baseflow <50L/s) and elevated baseline conductivity. Baseflow reaches a minimum in

early July and remains at these low levels until the beginning of December. During the summer

and fall streams respond rapidly to storm events, quickly reaching peak discharge before rapid

baseflow recession. The DCW site has large fluctuations in conductivity that coincide with

precipitation events (Figure 3.2.1b). These fluctuations are characterized by a large conductivity

increase at the onset of the storm event followed almost immediately by the dilution of surface

waters from precipitation. The range of conductivity over a single event period at the DCW site

may rise as high as 2000μS/cm and rapidly drop to 500μS/cm because of influence by the CC

tributary.

The SPNPO site is not subjected to conductivity increases at the onset of storm events

during this season, nor does it experience the range in conductivity that the DCW site does

(Figure 3.2.1). Conductivity values within this sub-basin are primarily controlled by the mixing of

low concentration surface water from storm events and higher concentration groundwater. This

produces the characteristic drop in conductivity at the beginning of a storm event followed by

the gradual return to higher baseline values (Figure 3.2.1a).

Baseline conductivity in Fuller Hollow Creek starts increasing in early May and reaches

its maximum in late September, coinciding with maximum soil moisture deficit. This suggests the

presence of a high TDS shallow groundwater reservoir that contributes to elevated stream

conductivity values in the Fall after evapotranspiration has depleted soil water stores. Baseline

conductivity at the SPNPO site continues to decline through winter and spring, interrupted by

large sudden increases in conductivity at the onset of precipitation events (Figure 3.2.1c). These

are interpreted to be flushing events likely from deicers applied to roadways in the upper

watershed. Conductivity becomes elevated at the DCW site for a period of several months

during the salting period and rapidly drops to a lower baseline for the spring months after a very large precipitation and snow melt event.
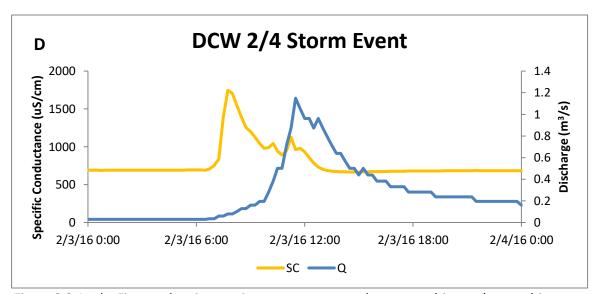
Figure 3.2.1a-d – Figures showing varying stream response between salting and non-salting seasons at the SPNPO and DCW site.

Stream TDS response to storm events during the winter season is opposite of the other seasons. Both less and more developed stream sites experience an increase in conductivity over the event period before returning to lower baseflow concentrations. This proves runoff has a higher TDS concentration than groundwater during this interval causing the rise in conductivity over the event period followed by a gradual dilution by groundwater to baseflow concentration (Figure 3.2.1). The transition between these two different response regimes can be sudden, as observed at the DCW site (Appendix I). The period of elevated stream conductivity abruptly ends after the 2/16 event, this event likely removed most of the salt deposition from urban surfaces and flushed soils with a large volume of melt water.

3.2.1 Cation Exchange Mechanisms for Pollutant Retention

Cation exchange is a naturally occurring process within soils where negatively charged sites on clays and organic matter adsorb and hold cations by electrostatic force, which may be exchanged by an influx of other cations. To confirm such an interaction in soils in the Fuller

Hollow Creek Watershed, a bivariate plot of Na:Cl concentrations from baseflow at three

locations along Fuller Hollow Creek (Figures 3.2.2a-f).

All three sites within Fuller Hollow Creek have a molar Na:Cl ratio of less than one, with

28%-30% of sodium absent from each site, assuming an initial 1:1 Na:Cl molar ratio (Eq. 3.3). In

order to determine that cation exchange is the primary factor influencing the Na:Cl imbalance,

Calcium, Potassium, and Magnesium concentrations were added to the measured Sodium

concentration then subtracted by the summation of the background value of each cation in an

attempt to achieve a 1:1 ratio with Cl (Figures 3.2.2a-f)(Eq. 3.4). Background values were

determined by plotting cation vs Cl milliequivalent concentrations and selecting a baseline

value, which was determined to be 0.65 mEq for each site. Since sorption is an electrostatic

reaction, milliequivalents were used to represent cations and anions (eq. 3.2).

Eq. 3.2

Millimolar Cation Exchange

$2Na^+ + Ca^{2+}(adsorbed) + 2K^+(adsorbed) + Mg^{2+}(adsorbed) \rightarrow Ca^{2+} + 2K + Mg^{2+} + 2Na^+(adsorbed)$

Eq. 3.3

Expected Relation with No Cation Exchange

$Na_{mEq} = Cl_{mEq}$

Eq. 3.4

Expected Relation with Cation Exchange

$Na_{mEq} + *Ca_{mEq} + *Mg_{mEq} + *K_{mEq} = Cl_{mEq}$
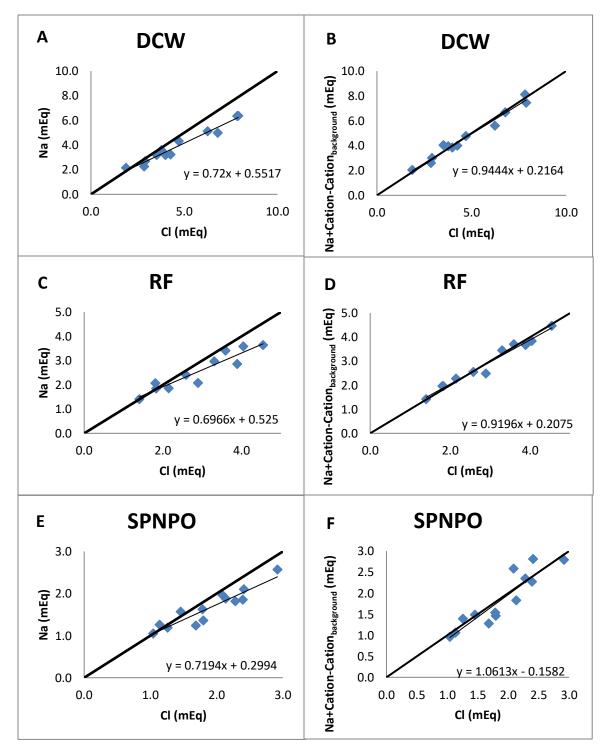
$Ca^{2+}mM = 0.5_{mEq}$ (*value after background correction)

$Mg^{2+}mM = 0.5_{mEq}$

mEq = milliequivalents
mM = millimolar

This correction produces a near 1:1 mEq ratio with chloride at each reach, suggesting cation exchange plays a significant role in influencing the aqueous geochemistry of groundwater in the Fuller Hollow Creek watershed. This finding also indicates that soils have not reached saturation with respect to sodium and will continue to adsorb and retain sodium ions until saturation has been achieved. Meriano et al. 2009 obtained similar results in a small Southern Ontario watershed impacted by road salting.

Alternative road salt storage methods in the subsurface include soil pore retention, where both Sodium and Chloride may be mechanically retained within soils (Kincaid and Findlay 2009). This storage method is more susceptible to being mobilized in first flush events (Robinson et al. 2017). Robinson et al. 2017 determined that sodium and chloride are typically retained in soils for a minimum of 2.5-5 months after salting, suggesting that soils are a significant pollutant reservoir that contribute to elevated Na and Cl concentrations year-round. This is consistent with conductivity increases at the onset of storm events observed within Fuller Hollow Creek during the non-salting seasons, interpreted to be a result of flushing of ions from soil micropores. Alternatively, this may represent flushing of atmospheric deposition to roadways and parking areas.

Figures 3.2.2a-f – Plots comparing Na/Cl ratios for each main stream site with Na plus additional cations vs Cl. The restoration of the expected near 1:1 Na/Cl mEQ ratio after addition of the major cations indicates the role of cation exchange within Fuller Hollow Creek soils.

3.2.2 Estimated Sodium and Chloride Retention Through Yearly Calculated Loads

Dissolved sodium and chloride loads were calculated at the outlet of each sub basin and the Fuller Hollow Creek watershed over the year-long study period. Calculated Na and Cl loads were compared to estimated atmospheric deposition and roadway application estimates to give the percentage of each ion retained within each watershed (Table 3.2). The amount of sodium retained ranges from 76% in the CC sub-basin to 23% in the SPNPO sub-basin. Chloride retention has a similar range of 76% at the CC sub-basin to just 9% at the SPNPO sub-basin. Percent of retained chloride loads are consistently less than sodium at all sites providing further evidence for a mechanism, such as cation exchange, that preferentially retains sodium.

Sites with higher impervious surface have less of a difference in retention between sodium and chloride, despite retaining more of these components overall. This suggests a significant portion of pollutant storage occurs through soil pore retention and storage in groundwater. Differences in sodium vs chloride retention at each site may be influenced by sodium saturation within soils in a cation exchange system.

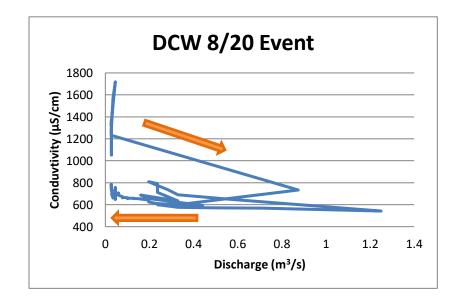|	Estimated Deposition (kg)	Measured Load (kg)	% Retained
Sodium			
DCW	632937	292351	54
SPNPO	110558	84889	23
CC	255481	60582	76
LLO	100588	62973	31
MHO	62672	20677	67
Chloride			
DCW	976064	557615	43
SPNPO	170493	154927	9
CC	393982	90871	74
LLO	155119	119319	15
MHO	96647	42544	56

Table 3.2- Estimated sodium and chloride deposition compared to observed chloride loads over the 1-year study interval.
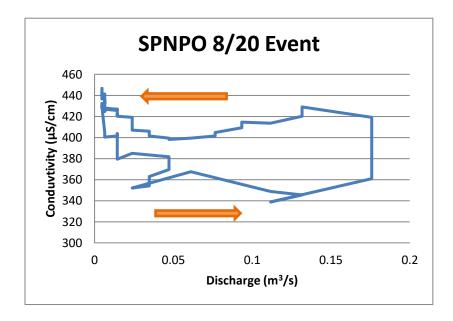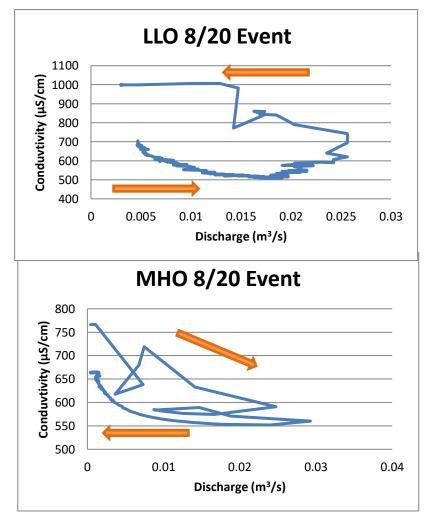
3.3 C/Q Hysteresis

The following analysis of six storm events attempts to determine the primary pollutant sources through C/Q hysteresis modeling. Three events from non-salting periods were selected in addition to three events from salting periods to determine if there was a change in primary pollutant source due to road salting. All of the events selected had a generally constant rate of precipitation, as variable or intermittent precipitation may influence hysteresis loop shape.

3.3.1 8/20/2015 Event

The 8/20 storm event occurs during the late summer pre-salting season, approximately 17.5 mm of rain precipitated over a 5-hour interval. The DCW Site is the only one which experiences a conductivity spike during the event. DCW, CC, and MHO sites all exhibit an Evans-Davies C3 type loop ($C_G > C_{SE} > C_{SO}$), while the LLO site exhibits a C1 type loop ($C_{SE} > C_G > C_{SO}$). The SPNPO site has a distinctive A1 type loop ($C_{SO} > C_G > C_{SE}$) which is expected from a suburban site during a non-salting season (Figure 3.3.1).

CC 8/20 Event
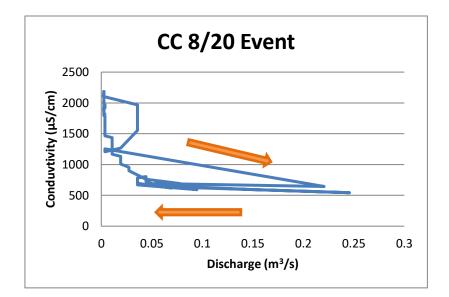
Figure 3.3.1- C/Q Hysteresis of the 8/20 storm event representing conditions during the non-salting season.

3.3.2 11/10/2015 Event

The 11/10 storm event captures a late fall, pre-salting, interval which precipitated approximately 50mm of rain over a 17-hour period resulting in similar hysteresis curves for all sonde sites (Appendix H). DCW and CC, exhibit a small conductivity spike at the onset of the event whereas the other three sites do not. All sites, however, exhibit an overall C3 type loop indicating $C_G > C_{SE} > C_{SO}$. The CC site has several smaller curves within the main C3 loop corresponding with various conductivity spikes throughout the event. This is likely due to the large storm sewer component of this site that drains various impervious surfaces, including parking lots, at different intervals throughout the event.

3.3.3 12/29/2015 Event
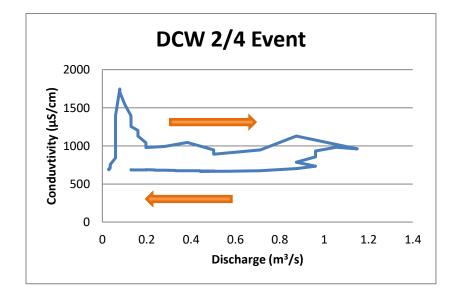
The 12/29 storm event captures a small winter event with approximately 10mm of precipitation over a 5-hour period. Rather than dilution and return to baseline values, all sites exhibit an increase in conductivity over the event period before returning to pre-event levels because of flushing from impervious surfaces. Both sites within the main channel of Fuller Hollow Creek (DCW and SPNPO) exhibit a C1 type loop indicating $C_{SE}>C_G>C_{SO}$. This behavior of a surface contaminant dominated system is expected in winter months with a large road salting component. The CC site exhibits a C3 type loop, which is counter intuitive, considering it is the most urbanized site, however as aforementioned, conductivity and discharge spikes seen throughout the event are likely due to the large parking lot and storm sewer components of this site. The tributary MHO and LLO sites both experience a C2 type event ($C_{SE}>C_{SO}>C_G$) (Appendix H).
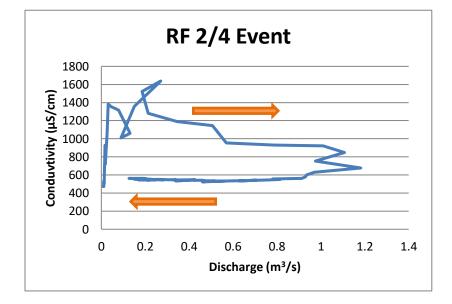
3.3.4 2/4/2016 Event
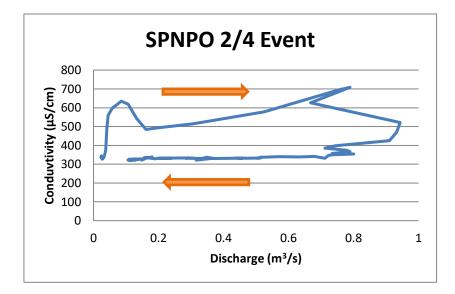
The 2/4 storm event captures a winter event with 17mm of precipitation over a 6.5-hour period. Increased conductivity is observed over the event period at all sites other than LLO and MHO. Rather than dilution and return to baseline values, all sites exhibit an increase in conductivity over the event period before returning to pre-event levels associated with flushing from impervious surfaces. All Fuller Hollow Creek main channel sites (DCW, RF, and SPNPO) exhibit a C1 type loop similar to the 12/29 event (Figure 3.3.2). The CC site exhibits a C3 type loop and is once again attributed to conductivity spikes throughout the event associated with variable storm sewer lag times. The LLO and MHO sites, do not experience a conductivity spike though the event, rather they experience a C3 and C1 type loop respectively. The C3 behavior of
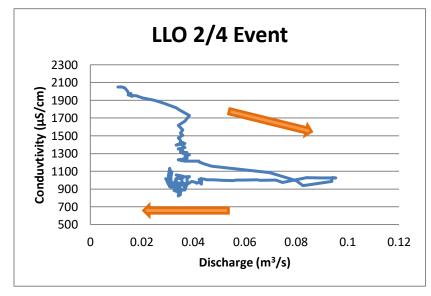
the LLO site is most probably due to the storage and dilution capacity of the retention pond

immediately prior to the site.

SPNPO 2/4 Event

MHO 2/4 Event

LLO 2/4 Event
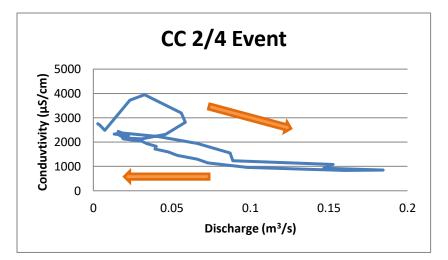
Figure 3.3.2- C/Q Hysteresis of the 2/4 storm event representing conditions during the salting season.
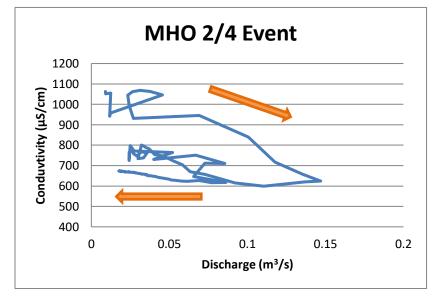
3.3.5 2/16/2016 Event

The 2/16 storm event captures a large winter event with approximately 40mm of precipitation over a 9-hour period. All sites have an increase in conductivity early in the event like the 12/29 storm. All sites exhibit a C3 type hysteresis loop, differing from the predicted C1 curves at main stream channel sites observed in the 12/29 event (Appendix H). This change in hysteresis pattern may be due to the large amount of snowmelt accompanying this event. Large amounts of snowmelt would continue to supply uncontaminated surface water throughout the event period, thus mimicking soil and groundwater hydrograph inputs when compared with other events.

3.3.6 5/6/2016 Event

The 5/6 event captures a late spring event precipitating 14mm over a 4-hour period. Most sites experience a small conductivity increase at the onset of the event before dilution except for the SPNPO site, which gradually increases in conductivity over the event period

(Appendix H). All sites show a C3 type hysteresis loop over the event period excluding the

SPNPO site which has an A1 type trend ($C_{SO}>C_G>C_{SE}$). The C3 trend is consistent with

expectations for late spring events which marks the beginning of evapotranspiration related

contributions to the increase in baseflow conductivity. The A1 trend at the SPNPO site, is

consistent with a rural stream response coupled with a small urban surface component.

3.3.7 Summary of Event Interpretations

C/Q hysteresis analysis of storm event from non-salting seasons at sites within the Fuller

Hollow Creek watershed primarily produced C3 type curves, contrary to the predicted A1 and A3

type curves (Table 3.3.1). Rose (2003) and Evans and Davies (1998) also observed C3 type curves

in non-salting periods and/or non-salting environments. Groundwater conductivity values to

event water being greater than surface and soil water suggests pollutant retention within

groundwater as well as evapotranspiration concentration over the summer and fall seasons,

corresponding to a negative water balance. An exception to this trend is the SPNPO site, where

an A1 type loop was dominant during the non-salting season. The limited impervious surface of

this sub-basin causes surface event water to be the lowest contributor and results in soil water

contributing more to stream conductivity than groundwater. This, along with cation exchange,

suggests a three-component pollutant storage model in the sub-surface is appropriate for road

salt contaminants. The 1st storage reservoir is electrostatic sites within soils which retain sodium

cations. The 2nd storage reservoir is soil micropores which retain both sodium and chloride ions

after infiltration. As these two reservoirs approach saturation, groundwater storage becomes

the third reservoir for infiltrating contaminants.

A combination of C1, C2, and C3 events were observed during salting seasons rather

than a consistent C3 pattern observed during non-salting season events (Table 3.3.1). Main

stream sites DCW, RF, and SPNPO differed in that they were dominated by C1 type curves, signifying surface water derived from urban runoff as the primary conductivity source. The C3 patterns observed during the 2/16 event at main stream sites may be due to the large amount of contaminated snowmelt from roadside locations accompanying this event. Large amounts of this contaminated snowpack would continue to melt throughout the event duration, thus mimicking soil and groundwater hydrograph inputs after peak discharge. The MHO site behaves like main stream sites during the salting season, with surface event water being the highest conductivity contributor, while conductivity sources vary in the other tributaries throughout the salting period.

The retention abilities of the Lake Liberman structure, immediately upstream from the LLO site, influence the C/Q hysteresis of this site during the salting season. The Lake Liberman retention pond mitigates the discharge and conductivity from storm events, removing or reducing road surface flushing associated with winter urban sites, and distributing pollutant loads and discharge over the event duration. This mitigation of components alters the distribution of the three-component hydrograph by effectively mixing components within the retention pond before discharging to the outlet site. Because of this feature the LLO site has a dominant C2/C3 nature in both salting and non-salting seasons.

The CC site maintains a C3 signature throughout the salting season as well. However, unlike the LLO site which mitigates conductivity during events, the CC site experiences very large increases in conductivity and discharge throughout the event duration. This is a direct result of lag times from the variable parking lot and storm sewer component of this sub-basin that drains campus surfaces. This makes the CC reach flashy in nature regarding both discharge and

conductivity. Because of the variability in lag times of surface event water superimposed over the soil and groundwater components, the three-component hysteresis model is deemed not applicable at CC.

C/Q Hysteresis Patterns						
Site	Salting			Non-Salting		
	29-Dec	4-Feb	16-Feb	20-Aug	10-Nov	6-May
DCW	C1	C1	C3	C3	C3	C3
RF	N/A	C1	N/A	N/A	N/A	C3
SPNPO	C1	C1	C3	A1	C3	A1
MHO	C2	C1	N/A	C3	C3	C3
LLO	C2	C3	C3	C1	C3	C3
CC	C3	C3	C3	C3	?	C3

Table 3.3.1- Evans-Davies classification hysteresis loop types for each site and storm event. "N/A" indicates no data available, "?" indicates no definitive loop

3.4 INCA-Cl Results:

The INCA-Cl model utilizes landcover, soil moisture, precipitation, and chloride deposition data to simulate stream discharge and chloride concentrations in daily increments over the modeled period. INCA-Cl calculates surface runoff, soil water, and groundwater contributions in order to simulate the daily stream discharge and chloride concentrations at each modeled site. INCA-Cl model inputs for this study are found in Appendix I.

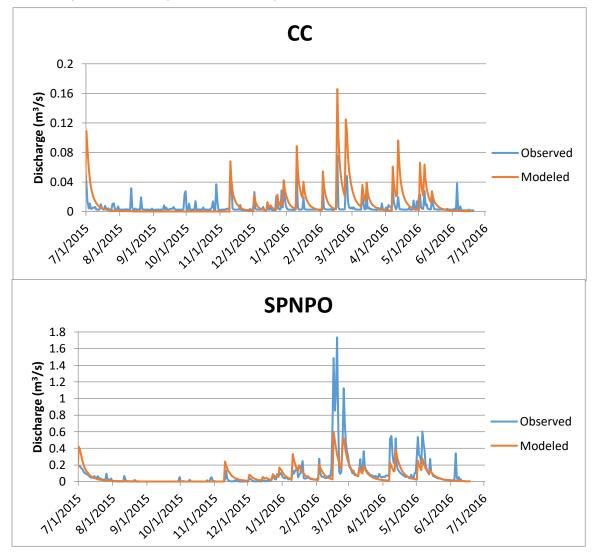Observed and modeled discharge at each of the main stream sites correlate reasonably well, with r^2 values ranging from 0.56 to 0.66 (table 3.4.1). Due to the large impervious surface component in the watershed, and near ubiquitous fragipan layer preventing infiltration (Broome County Soil Survey 1971), streams were generally flasher and saw a return to baseflow more quickly than could be predicted by the model.

Observed vs Modeled Q		Observed vs Modeled Cl	
Site	r^2	Site	r^2
DCW	0.66	DCW	0.35
RF	0.56	RF	0.05
SPNPO	0.59	SPNPO	0.24
MHO	.06	MHO	0.02
LLO	0.39	LLO	0.03
CC	0.31	CC	0.20

Table 3.4.1- r^2 values of INCA-Cl modeled discharge and chloride concentrations. While r^2 may not be the best statistical method for correlation analysis, it's ubiquity allows some insight into modeling accuracy. Methods, such as Willmott's index of agreement, may be better suited for determining correlation with observed results.

The results for chloride concentrations within the main stream were less well modeled than discharge. The DCW and SPNPO sites have the highest correlation with an r^2 of 0.35 and 0.24 respectively. The highest correlation at these two sites is due to the lack of large fluctuations in chloride from flushing events due to the large non-urban percentage of landcover at these sites (Appendix I). Due to the complex runoff from impervious surfaces and the inherent simplicity of the INCA-Cl model, large conductivity increases from urban flushing events are not accurately represented in the modeling scenarios. At present, INCA-Cl distributes chloride deposition over the entire watershed area rather than scaling deposition to proximity to roadways. By confining road salt deposition to urban landcover, model parameters of residence times and initial flow velocity may be altered to better fit observed results. Applying chloride deposition equally over the entire watershed may be acceptable in a larger and more homogenous watershed, but in the small and highly urbanized Fuller Hollow Creek watershed this feature creates discrepancies between modeled and observed results. The INCA-Cl model does however accurately represent baseline chloride conditions within the watershed as well as

fresh water dilution from storm events (Figure 3.4.1). INCA-Cl can also predict the chloride

increase over an event period followed by recession to baseflow values during the winter

months at the DCW, RF, and SPNPO sites. This result is consistent with C/Q hysteresis models

which identified surface water as the largest contributor to dissolved stream loads during the

salting season.

While INCA-Cl can reasonably predict chloride values within Fuller Hollow Creek, values

within the 1st order tributaries do not correlate as well with observed results (Appendix I). This is

likely due to the infrastructure in each tributary, ranging from large storm sewer components to

retention ponds which requires a more complex model to simulate.
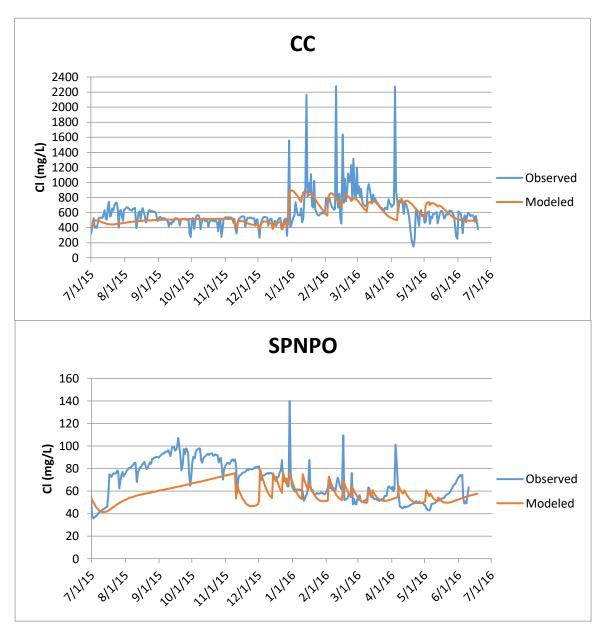
Figure 3.4.1- Modeled and observed discharge and chloride concentrations of the CC and SPNPO sites representing an urban and sub-urban sub-watershed response in the Fuller Hollow Creek Watershed.
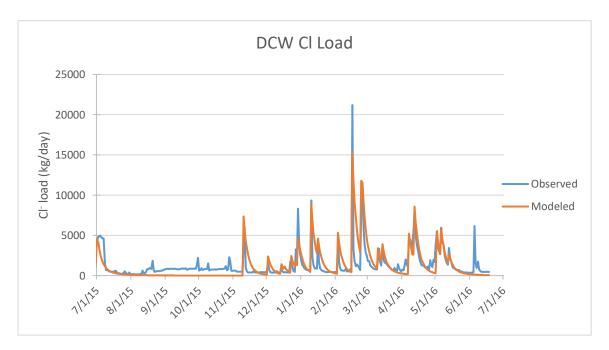
3.4.1 Chloride Loads

Chloride load estimates from each site represent the model's combined ability to estimate coupled discharge and chloride concentrations (Figure 3.4.2). Model results are lower than observed loads, except at the CC and MHO sites where underestimated low-flow discharge resulted in a lower total chloride load (Table 3.4.2). r^2 values of loads from main stream sites,

which have the highest discharge correlation, range from 0.49 to 0.54. Lower modeled values of

chloride loads are mainly due to the model inability to accurately estimate impervious surface

flushing during storm events and modeled baseflow discharge being less than observed values.

Observed vs Modeled Loading Results			
Site	Observed (kg/year Cl)	INCA-Cl (kg/year Cl)	Percent of Observed
DCW	529723	473740	89.4
SPNPO	152432	118890	80.0
MHO	42981	62027	144.3
LLO	131339	89770	68.4
CC	103185	250815	243.0

Observed vs Modeled Loading r^2	
Site	r^2
DCW	0.49
SPNPO	0.54
MHO	0.1
LLO	0.28
CC	0.46

Table 3.4.2- Observed chloride loads compared to modeled INCA-Cl chloride loads and accompanied r^2 values of modeled chloride loads.
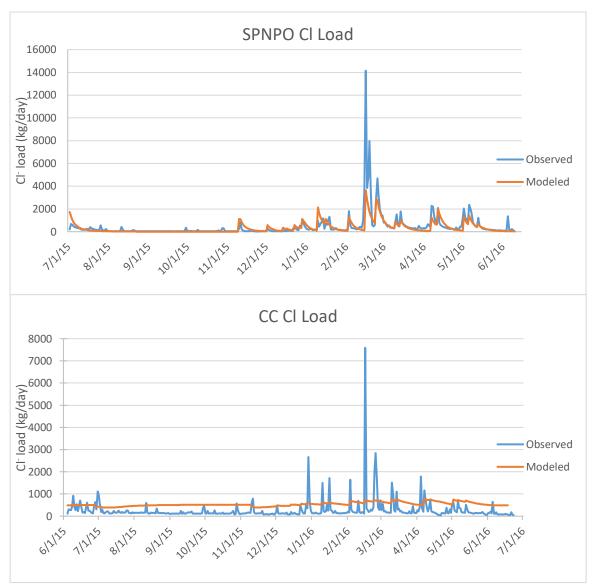
Figure 3.4.2- Modeled and observed chloride loads of the DCW, SPNPO, and CC sites representing the total watershed, sub-urban, and urban watershed chloride export throughout the study period.

3.4.2 Alternative Deposition Scenarios

By adjusting depositional amount to the Fuller Hollow Creek watershed, the INCA-Cl model can predict how stream chloride concentrations will react to those changes. Several different depositional scenarios were input to the model to ascertain changes to chloride concentrations and loads after a 50% reduction and 50% addition to chloride deposition (Figure 3.4.3). A 50% reduction in chloride deposition to the Fuller Hollow Creek watershed would lead to a 28% immediate reduction in chloride loads over the study period. A 50% increase in chloride deposition would lead to a 24% increase in chloride loads over the study period. Modeled chloride levels under variable loading conditions have identical values during the summer period due to the model only including groundwater contributions over this period. Over many seasons the groundwater concentration would gradually increase or decrease dependent on long term changes to salt application rates to roadways, however over the yearly modeled period these systems are still dependent on the existing groundwater concentrations.
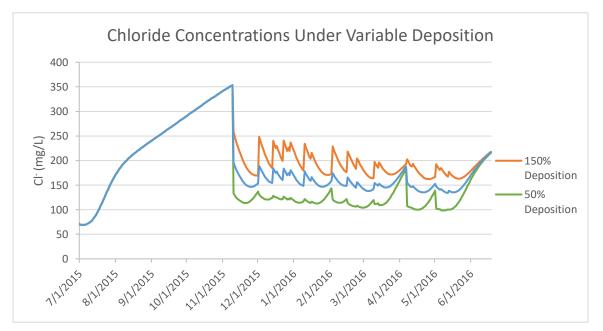

Figure 3.4.3- Modeled chloride concentrations at the DCW site under variable deposition scenarios. These results also indicate the sensitivity of the model to inaccuracies in salt application rate estimates.

Chapter 4 Conclusions

4.1 Long Term Trends

Levels of total dissolved solids within streams have increased at all sub-basin stream sites within the Fuller Hollow Creek Watershed over the past 10 years. Total dissolved solids within streams also correlate with the amount of impervious surface in each sub-basin with TDS levels increasing by 33mg/L for every percent increase in impervious surface. However, rates of Increase were not explainable by an increase in the amount of impervious surface over the study period alone. Levels of all major cations also correlate with impervious surface percentage. Sodium concentrations have substantially increased at all stream sites. Sodium was the most abundant cation, and had the highest rate of increase, with higher rates of increase in the spring at tributary sites versus main channel sites. Despite an overall increase in stream water TDS, two of the four groundwater wells sampled showed no conclusive TDS increase because high conductivity surface runoff infiltration was confined to shallow preferential flow paths.

4.2 Pollutant Storage

Cation exchange in soil is a factor in retaining sodium from road salt deposition. This became less of a factor in sub-basins with higher NaCl deposition and suggests soil reservoirs may be near saturated with respect to sodium. In the non-salting season, C/Q hysteresis plots indicate groundwater is the dominant conductivity contributor ($C_G > C_{SE} > C_{SO}$) at all sites except SPNPO where soil water is the dominant conductivity contributor ($C_{SO} > C_G > C_{SE}$). During the

salting season all site's response to storm events are dominated by surface water contribution, with main stream sites having a secondary contribution from groundwater ($C_{SE}>C_G>C_{SO}$) and tributaries a mix of groundwater and soil water as secondary conductivity contributors ($C_{SE}>C_{SO}>C_G$). C/Q hysteresis results from the CC site were inconclusive due to the large parking lot surface and storm sewer network of that sub-basin which influenced discharge lag times.

4.3 INCA-Cl

INCA-Cl was able to accurately model stream discharge and baseline chloride trends within the Fuller Hollow Creek Watershed, with greater success in the main stream channel than the smaller tributaries. INCA-Cl was unable to model large chloride increases associated with flushing events from impervious surfaces due to the way the modeled chloride deposition is distributed across the entirety of the watershed and the flashy nature of the storm response in the watershed. By increasing or decreasing the chloride deposition to the watershed by 50%, an immediate 28% reduction or 24% increase in chloride levels were predicted.

Chapter 5 Future Work

5.1 Historical Data

The continuation of groundwater and stream water sampling within the Fuller Hollow Creek watershed by Binghamton University students would continue to provide data on long-term stream and groundwater conditions. These analyzed samples provide an archive of data that may be utilized to assess predictions of future contaminant accumulation, and more accurately quantify the effects of road salt pollution. Multi-site long term stream and groundwater geochemistry archives is generally rare and provides a unique opportunity for future studies in this mixed landuse watershed.

5.2 Sonde Data

To better discern conditions within the Fuller Hollow Creek Watershed, more accurate discharge measurements may be necessary. The CC site was subject to underestimated low-flow data due to use of the existing weir for discharge calibration. McCann (2013) determined the best fit weir equation for this site, however under low flow conditions calibration becomes increasingly difficult to assess. Better rating curve calibration at the MHO site would also improve observational quality, as this site was prone to sonde burial and dislodgement.

Better quantification of sonde calibration during high discharge events at all sites would also improve the accuracy of calculated hydrographs. The flashy nature of the watershed makes it difficult to capture these high-discharge events due to timing and safety constraints. Continued

monitoring at the DCW site sonde is advocated so that long term changes in discharge and chloride may be modeled in the future.

5.3 INCA-Cl

Applying the INCA-Cl model to other regional watersheds would allow for the continued assessment and refinement of the INCA-Cl model, as well as to compare the effects of road salt deposition under varying conditions. We tried to apply INCA-Cl to the Apalachin creek watershed using the parameters calibrated for the Fuller Hollow Creek Watershed. The Apalachin Creek Watershed is a 112.6 km^2 watershed located approximately 15.5 km west of the Fuller Hollow Creek watershed. Data from the Apalachin Creek Watershed Is collected and compiled by the Susquehanna River Basin Commission (SRBC) and includes stream conductivity, temperature, and dissolved oxygen levels. The lack of stage measurement and large agricultural component and low urban component relative to the FHC watershed made the calibration for the Apalachin creek watershed incompatible (figure 5.3.1). Due to no discharge component being collected, calibrating modeled discharge was not possible.

The INCA-Cl model has also been used to simulate long-term, multi-decade, chloride concentrations under changing climate conditions (Gutchess et. al 2018). A similar scenario could be applied to the Fuller Hollow Creek Watershed and be refined using archived historical data and continued stream monitoring using sondes.
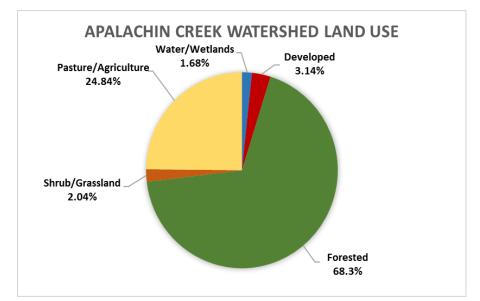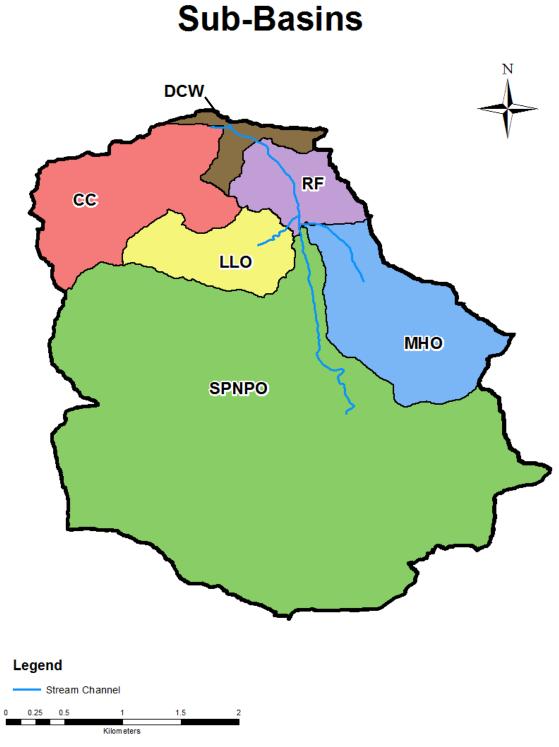
Figure 5.3.1- Apalachin Creek watershed landcover used for input to the INCA-Cl model (NLCD 2011). The Apalachin creek watershed differs from Fuller Hollow Creek in that it has a large agricultural component and small urban surface percentage, opposite of Fuller Hollow Creek.

Appendices
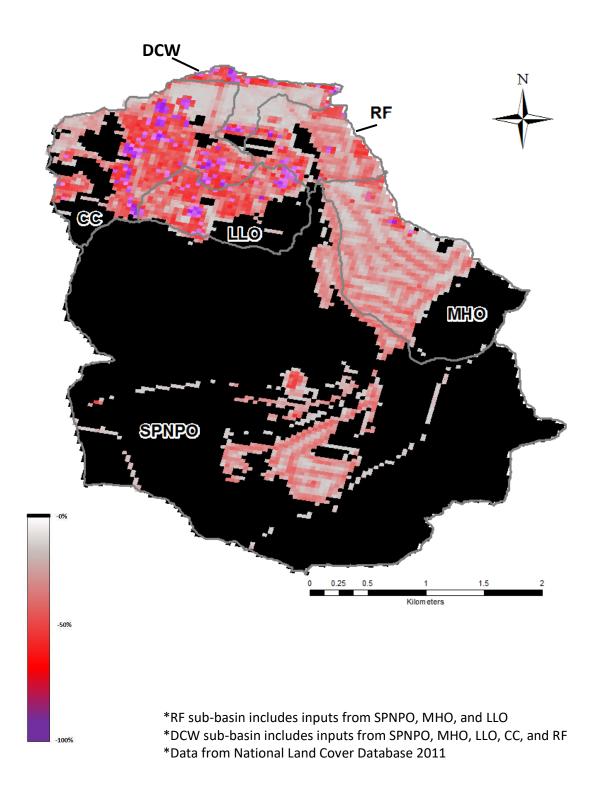
Appendix A

Fuller Hollow Creek Maps
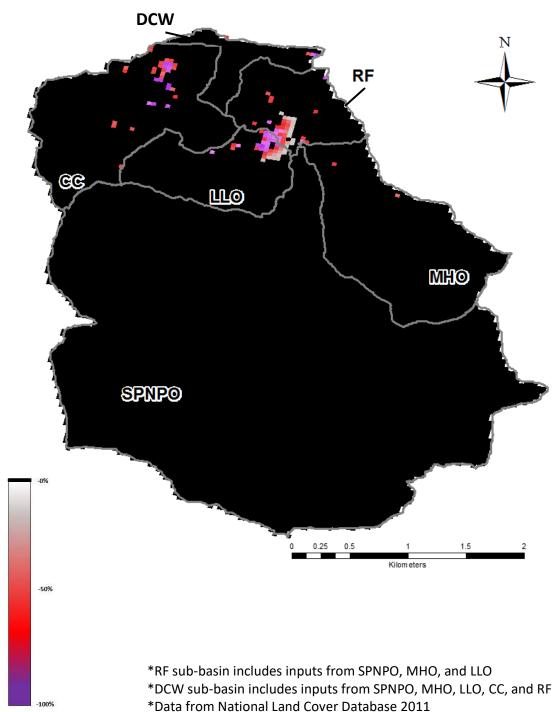
Sub-Basins

*RF sub-basin includes inputs from SPNPO, MHO, and LLO
*DCW sub-basin includes inputs from SPNPO, MHO, LLO, CC, and RF

Impervious Surface 2011

*RF sub-basin includes inputs from SPNPO, MHO, and LLO
*DCW sub-basin includes inputs from SPNPO, MHO, LLO, CC, and RF
*Data from National Land Cover Database 2011

Impervious Surface Change
2006-2011

*RF sub-basin includes inputs from SPNPO, MHO, and LLO
*DCW sub-basin includes inputs from SPNPO, MHO, LLO, CC, and RF
*Data from National Land Cover Database 2011

INCA-CI Land Cover

Legend

- Forested
- Short Vegitation
- Agricultural
- Urban

*RF sub-basin includes inputs from SPNPO, MHO, and LLO
*DCW sub-basin includes inputs from SPNPO, MHO, LLO, CC, and RF
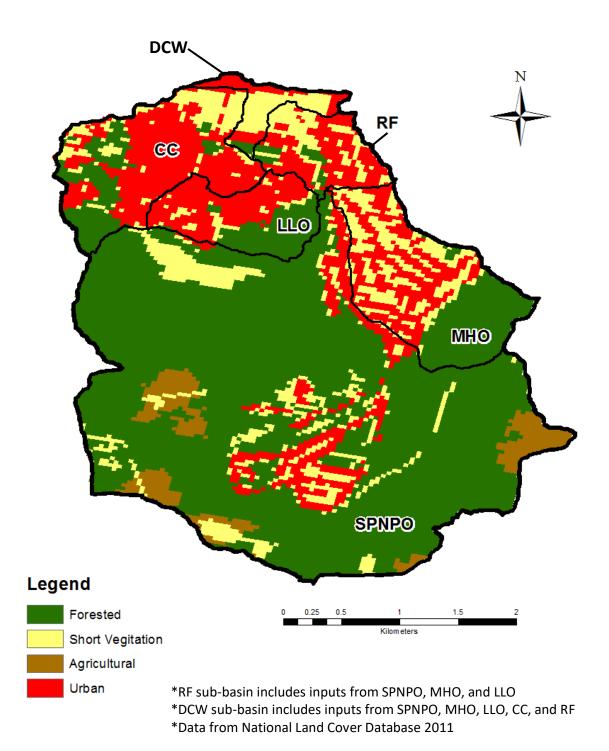*Data from National Land Cover Database 2011
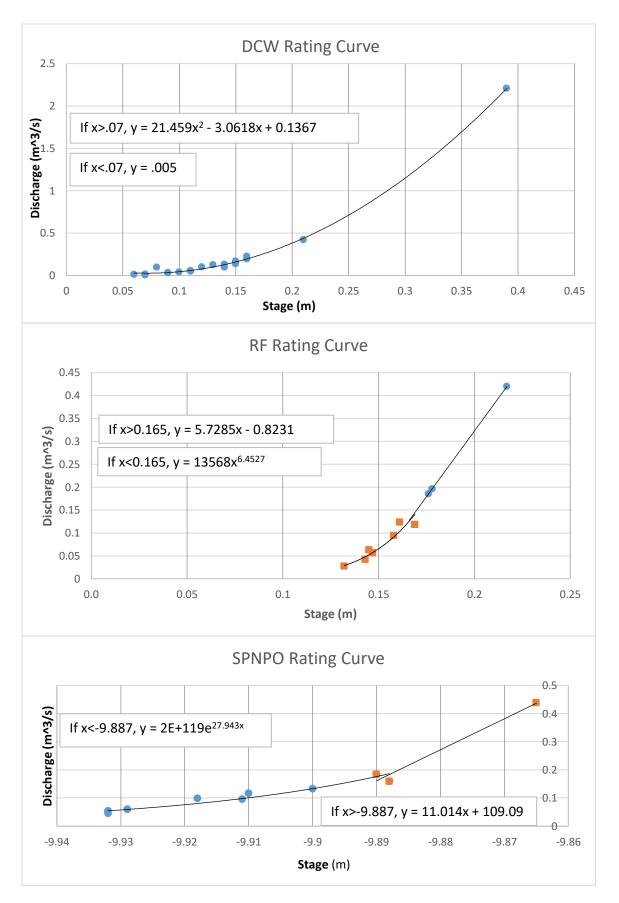
Appendix B

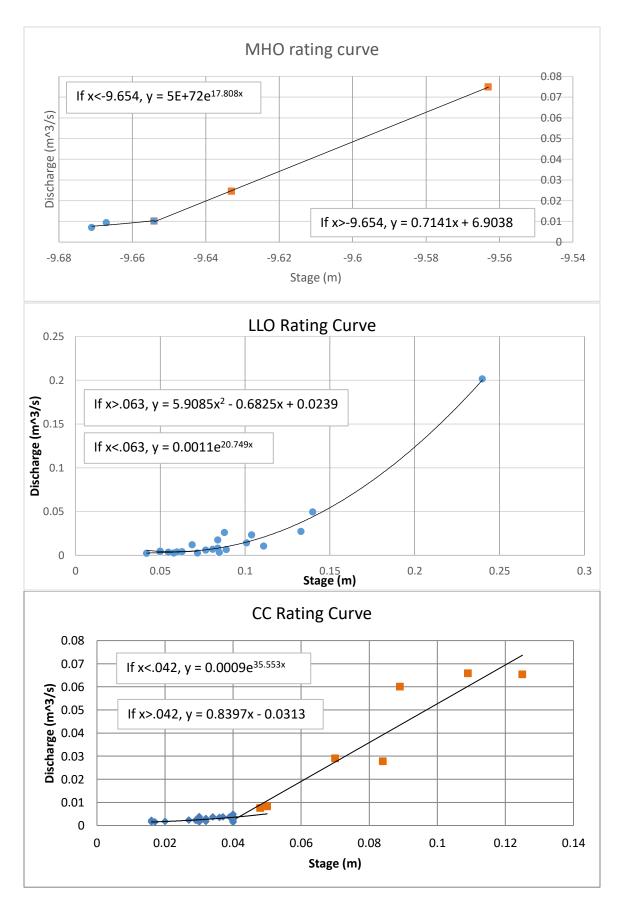Stream Sonde and Groundwater Well Locations and Descriptions

Sonde Locations	Description
DCW: (42° 5'45.34"N, 75°57'56.06"W)	Located approximately 0.35km upstream of Fuller Hollow Creek's confluence with the Susquehanna River. Includes all inputs from subsequent sites.
CC: (42° 5'42.73"N, 75°57'58.70"W)	Located in drainage ditch along the 4 lane Vestal Parkway. Most discharge is from two storm sewer culverts that drain a large portion of the Binghamton University Campus.
RF: (42° 5'39.01"N, 75°57'48.42"W)	Located within the northern portion of Fuller Hollow Creek and represents stream conditions prior to input from the CC sub-basin.
LLO: (42° 5'15.09"N, 75°57'39.66"W)	Located at the outlet of the Lake Liberman retention pond that accumulates runoff from the Binghamton University Campus then discharging into Fuller Hollow Creek.
MHO: (42° 5'15.26"N, 75°57'34.85"W)	Located within 1st order stream that drains a large residential, suburban area east of the Binghamton University campus before intersecting Fuller Hollow Creek.
SPNPO: (42° 5'14.33"N, 75°57'36.19"W)	Site located approximately 30m upstream of MHO site in main stream channel, inputs include a few suburban areas and large rural/ natural areas in the southern regions of the watershed.

Well Locations	Description
RFW (42° 5'40.12"N, 75°57'52.77"W)	12.2m deep well with opening in surficial glacial aquifer. Steel casing.
MSW (42° 5'33.49"N, 75°57'45.07"W)	9.1m deep well at corner of parking lot with casing at ground level. Opening to surficial glacial aquifer. Steel casing.
CDW (42° 5'22.10"N, 75°57'38.69"W)	37m deep well with opening to shale bedrock of the Upper Walton Formation. Steel casing
NSW (42° 5'22.62"N, 75°57'38.80"W)	6.7m well with opening in surficial glacial aquifer. PVC casing.
SSW (42° 5'22.02"N, 75°57'38.25"W)	6.7m well with opening in surficial glacial aquifer. PVC casing.

Appendix C
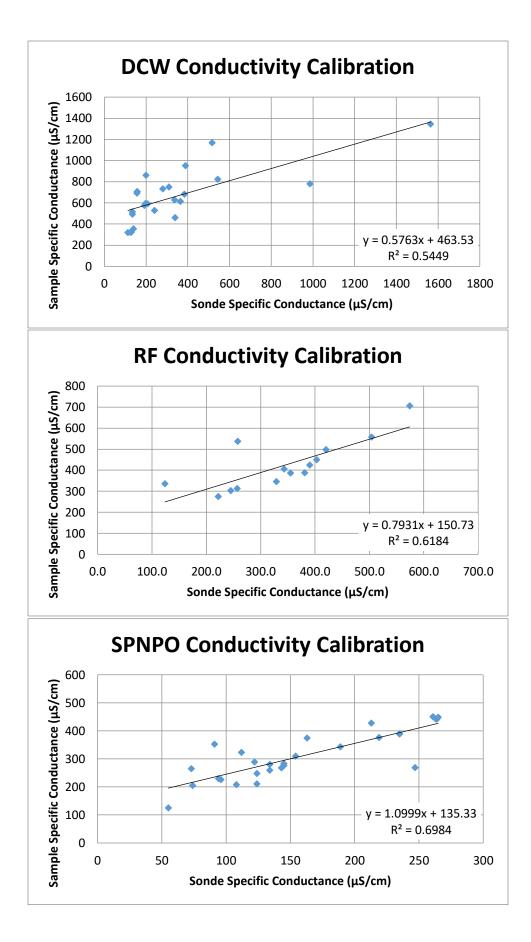
Stream Sonde Rating Curves

DCW Rating Curve

If x>.07, y = 21.459x^2 - 3.0618x + 0.1367

If x<.07, y = .005

RF Rating Curve

If x>0.165, y = 5.7285x - 0.8231

If x<0.165, y = 13568x$^{6.4527}$

SPNPO Rating Curve

If x<-9.887, y = 2E+119e$^{27.943x}$

If x>-9.887, y = 11.014x + 109.09

MHO rating curve

If x<-9.654, y = 5E+72e^{17.808x}

If x>-9.654, y = 0.7141x + 6.9038

Discharge (m^3/s)

Stage (m)

LLO Rating Curve

If x>.063, y = 5.9085x² - 0.6825x + 0.0239

If x<.063, y = 0.0011e^{20.749x}

Discharge (m^3/s)

Stage (m)

CC Rating Curve

If x<.042, y = 0.0009e^{35.553x}

If x>.042, y = 0.8397x - 0.0313
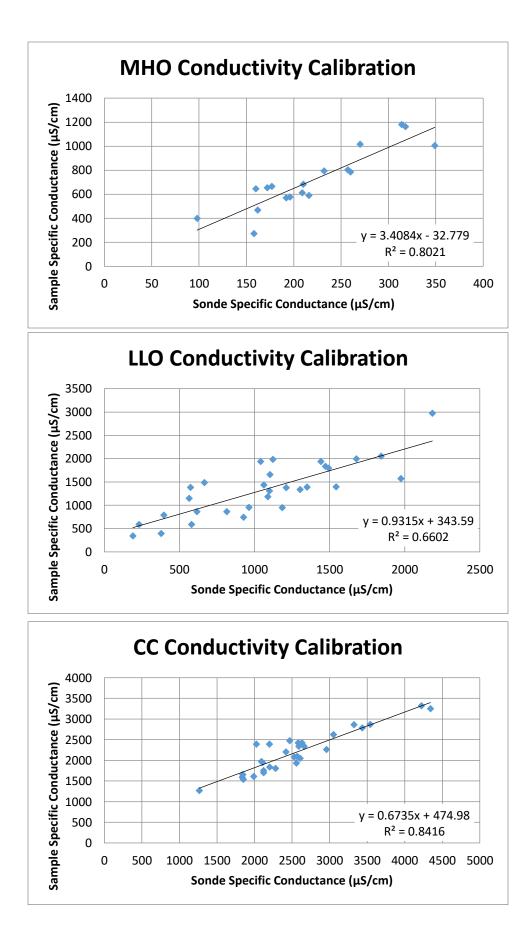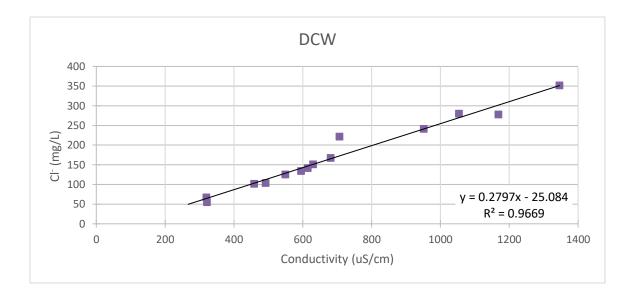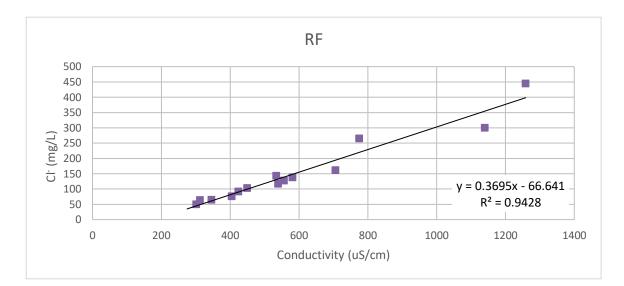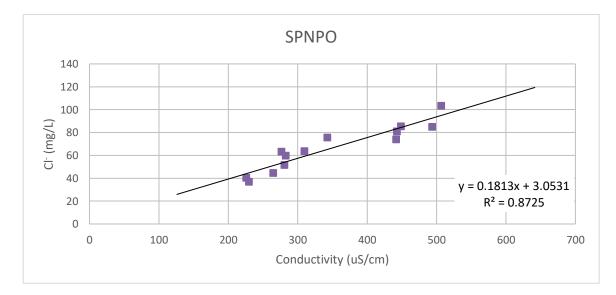
Discharge (m^3/s)

Stage (m)

Appendix D

Stream Sonde Conductivity and Dissolved Ion Calibration

DCW Conductivity Calibration

y = 0.5763x + 463.53
R² = 0.5449

RF Conductivity Calibration

y = 0.7931x + 150.73
R² = 0.6184

SPNPO Conductivity Calibration

y = 1.0999x + 135.33
R² = 0.6984

MHO Conductivity Calibration

y = 3.4084x - 32.779
R² = 0.8021

LLO Conductivity Calibration

y = 0.9315x + 343.59
R² = 0.6602

CC Conductivity Calibration

y = 0.6735x + 474.98
R² = 0.8416

DCW

y = 0.2797x - 25.084
R² = 0.9669

RF

y = 0.3695x - 66.641
R² = 0.9428

SPNPO

y = 0.1813x + 3.0531
R² = 0.8725

LLO

y = 0.2933x - 29.389
R² = 0.924

MHO

y = 0.3097x - 59.495
R² = 0.8987

CC

y = 0.2969x - 48.639
R² = 0.8886

DCW

y = 0.1419x - 6.8786
R² = 0.9406

RF

y = 0.114x + 4.3659
R² = 0.941

SPNPO

y = 0.0869x + 5.3849
R² = 0.8301

DCW

y = 0.071x - 4.0002
R² = 0.8747

RF

y = 0.0686x - 1.6088
R² = 0.906

SPNPO

y = 0.1114x - 10.924
R² = 0.9253

LLO

y = 0.0459x + 10.979
R² = 0.7101

MHO

y = 0.0506x + 19.506
R² = 0.3773

CC

y = 0.0275x + 49.034
R² = 0.3265

Appendix E

INCA-Cl Model Input

Soil Moisture Deficit and Hydrologically Effective Rainfall

INCA-Cl Input Parameters						
Basin	DCW	RF	SPNPO	MHO	LLO	CC
Area (km^2)	9.59	8.30	6.20	1.11	0.55	1.07
Reach Length (m)	2950	2650	1817	730	500	1545
Land Cover Classification (%)						
Forested	59.4	65.4	77.2	35.0	36.3	23.1
Short Veg.	15.1	13.6	9.6	30.3	9.3	20.4
Arable	4.1	4.7	6.2	0.0	0.0	0.0
Urban	21.4	16.4	7.0	34.7	54.4	56.5
Baseflow Index	0.1	0.1	0.2	0.5	0.1	0.1
Flow Parameter "a"	10	10	10	10	10	10
Flow Parameter "b"	0.7	0.7	0.7	0.2	0.7	0.7
Land Cover Parameters						
Forested						
Soil Water						
Residence Time (days)	5	5	5	5	5	5
Initial Flow (m^3/s)	0.1	0.1	0.1	0.1	0.1	0.1
Initial Chloride Concentration (mg/L)	20	20	20	20	20	20
Groundwater						
Residence Time (days)	15	15	15	15	15	15
Initial Flow (m^3/s)	0.01	0.01	0.01	0.01	0.01	0.01
Initial Chloride Concentration (mg/L)	15	15	15	15	15	15
Short Veg.						
Soil Water						
Residence Time (days)	1	1	1	1	1	1
Initial Flow (m^3/s)	0.06	0.06	0.06	0.06	0.06	0.06
Initial Chloride Concentration (mg/L)	200	200	200	200	200	200
Groundwater						
Residence Time (days)	20	20	20	20	20	20
Initial Flow (m^3/s)	0.06	0.06	0.06	0.06	0.06	0.06
Initial Chloride Concentration (mg/L)	200	200	200	200	200	200
Arable						
Soil Water						
Residence Time (days)	3	3	3	3	3	3
Initial Flow (m^3/s)	0.10	0.10	0.10	0.10	0.10	0.10
Initial Chloride Concentration (mg/L)	150	150	250	150	150	150
Groundwater						
Residence Time (days)	15	15	15	15	15	15
Initial Flow (m^3/s)	0.06	0.06	0.06	0.06	0.06	0.06
Initial Chloride Concentration (mg/L)	200	200	200	200	200	200
Urban						
Soil Water						
Residence Time (days)	4	4	3.5	3.5	4	4
Initial Flow (m^3/s)	0.50	0.50	0.50	0.50	0.50	0.50
Initial Chloride Concentration (mg/L)	200	200	200	400	800	800
Groundwater						
Residence Time (days)	18	18	17	16	18	18
Initial Flow (m^3/s)	0.05	0.05	0.05	0.05	0.05	0.05
Initial Chloride Concentration (mg/L)	750	750	350	350	750	750

Soil and Groundwater Flow Models

Soil zone : $\dfrac{dx_1}{dt} = \dfrac{1}{T_1}(U_1 - x_1)$

Groundwater : $\dfrac{dx_2}{dt} = \dfrac{1}{T_2}(U_2 x_1 - x_2)$

Relationship Between Inflow, Outflow, and Storage

$$\dfrac{dS(t)}{dt} = I(t) - Q(t)$$

$$S(t) = T(t) \times Q(t)$$

Travel Time Parameter

$$T(t) = \dfrac{L}{v(T)}$$

Relationship Between Flow Velocity and Discharge

$$v(t) = aQ(t)^b$$

Chloride Mass Balance in Soil and Groundwater

Soil zone : $\dfrac{dc_1}{dt} = \dfrac{1}{V_1}(U_3 - x_1 c_1)$

Groundwater zone : $\dfrac{dc_2}{dt} = \dfrac{1}{V_2}(U_2 x_1 c_1 - x_2 c_2)$

Chloride Mass Balance in Stream Reach

Flow : $\dfrac{dQ_d}{dt} = \dfrac{1}{T_3}(Q_u - Q_d)$

Chloride : $\dfrac{dC_d}{dt} = \dfrac{1}{V_3}(Q_u C_u - Q_d C_d)$

Where $V_3 = T_3 Q_d$ and $T_3 = \dfrac{L}{v} = \dfrac{L}{aQ^b}$

I= Inflow
Q= Outflow
S= Storage
T=Travel time parameter (days)
L= Reach length (m)
V= mean flow velocity (m/s)
X= flow in soil and groundwater (m^3/s)
a+b= Flow constants
c= Daily chloride concentrations (mg/L)
U_2= Baseflow Index
V= Water volumes for soil and groundwater zones (m^3)
U_3= Daily chloride loading (kg)
$_u$ = upstream
$_d$ =downstream
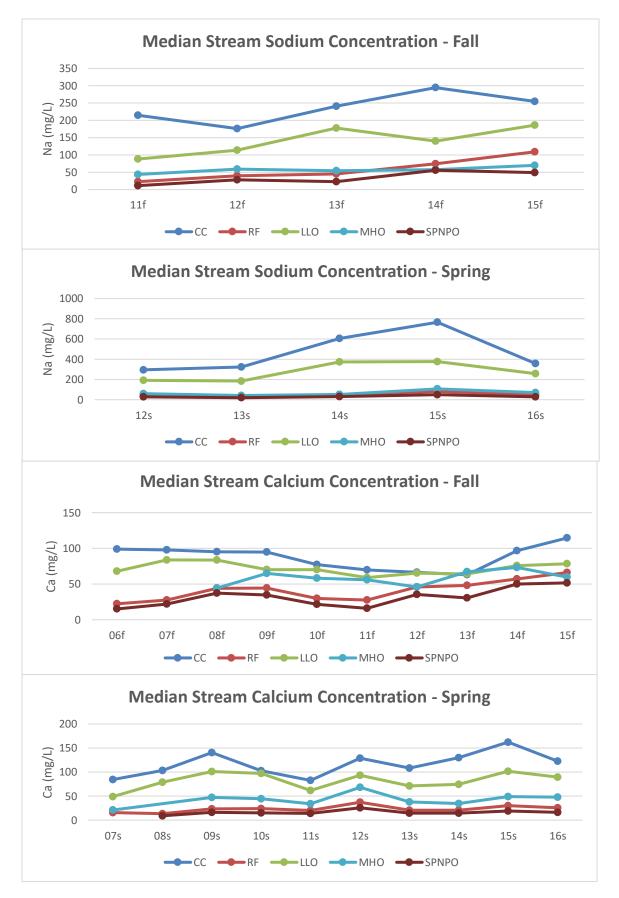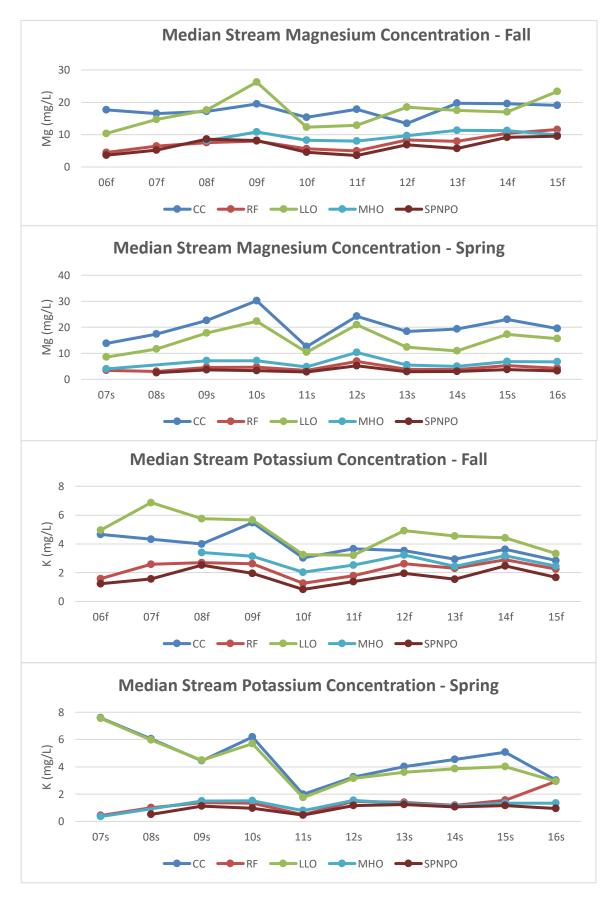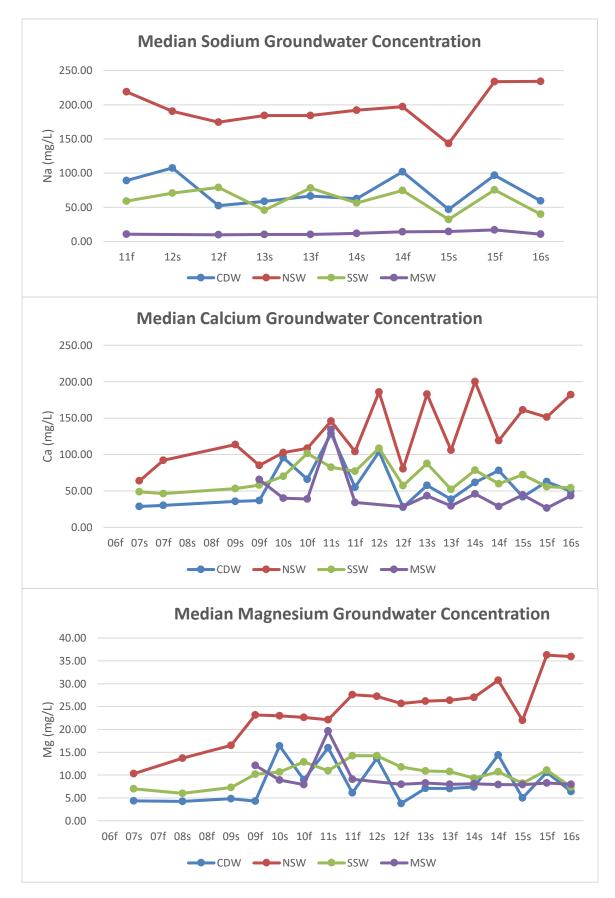
Appendix F
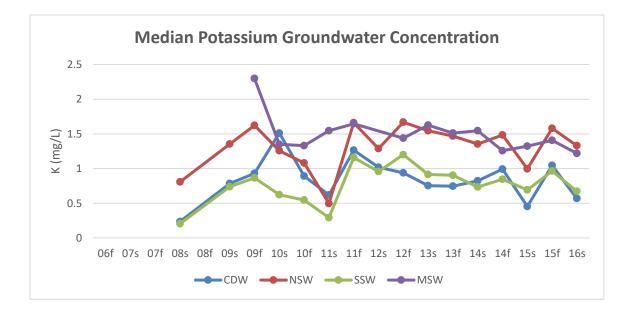
Long Term Stream and Groundwater Data

Note: The change in analytical method is evident for some of the measured sodium cations. The increase in Na, for sample sites consistently over 100mg/L post spring 2011, is attributed to false low readings, obtained with the DCP, from samples exceeding its detection limits. Due to this feature all sodium data prior to fall 2011 was omitted from analysis.

Median Stream Sodium Concentration - Fall

Median Stream Sodium Concentration - Spring

Median Stream Calcium Concentration - Fall

Median Stream Calcium Concentration - Spring

Median Stream Magnesium Concentration - Fall

Median Stream Magnesium Concentration - Spring

Median Stream Potassium Concentration - Fall

Median Stream Potassium Concentration - Spring

Median Sodium Groundwater Concentration

A line chart titled "Median Sodium Groundwater Concentration" plotting Na (mg/L) on the y-axis (0.00 to 250.00) against time periods on the x-axis (11f, 12s, 12f, 13s, 13f, 14s, 14f, 15s, 15f, 16s) for series CDW, NSW, SSW, and MSW.

Median Calcium Groundwater Concentration

A line chart titled "Median Calcium Groundwater Concentration" plotting Ca (mg/L) on the y-axis (0.00 to 250.00) against time periods on the x-axis (06f, 07s, 07f, 08s, 08f, 09s, 09f, 10s, 10f, 11s, 11f, 12s, 12f, 13s, 13f, 14s, 14f, 15s, 15f, 16s) for series CDW, NSW, SSW, and MSW.

Median Magnesium Groundwater Concentration

A line chart titled "Median Magnesium Groundwater Concentration" plotting Mg (mg/L) on the y-axis (0.00 to 40.00) against time periods on the x-axis (06f, 07s, 07f, 08s, 08f, 09s, 09f, 10s, 10f, 11s, 11f, 12s, 12f, 13s, 13f, 14s, 14f, 15s, 15f, 16s) for series CDW, NSW, SSW, and MSW.

Median Potassium Groundwater Concentration

Stream Dissolved Cation Increase/ Year, Spring			
Site	Sodium (mg/L/year)	Calcium (mg/L/year)	Magnesium (mg/L/year)	Potassium (mg/L/year)
CC	56.7	4.7	0.3	-0.3
LLO	32.7	2.1	0.3	-0.4
MHO	8.6	1.7	0.1	0.1
RF	6.1	1.2	0.1	0.2
SPNPO	3.1	0.6	0	0

Stream Dissolved Cation Increase/ Year, Fall			
Site	Sodium (mg/L/year)	Calcium (mg/L/year)	Magnesium (mg/L/year)	Potassium (mg/L/year)
CC	19.9	-0.7	0.2	-0.2
LLO	22.2	-0.5	0.7	-0.2
MHO	5.1	2.0	0.3	-0.1
RF	20.7	3.8	0.6	-0.1
SPNPO	10.3	2.9	0.4	0

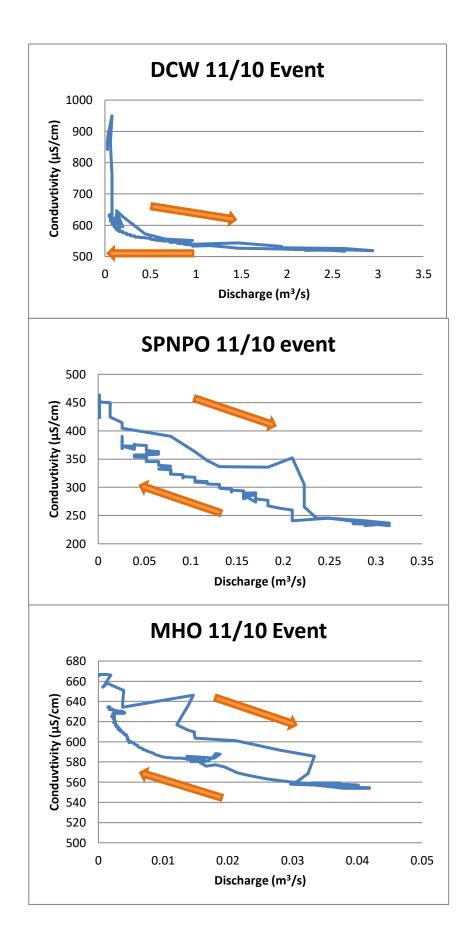| Groundwater Dissolved Cation Increase/ Year			
Site	Sodium (mg/L/year)	Calcium (mg/L/year)	Magnesium (mg/L/year)	Potassium (mg/L/year)
CDW	-2.9	1.6	0.3	0
NSW	4.0	10.4	2.2	0
SSW	-3.7	0.8	0.2	0
MSW	1.1	-5.0	-0.7	-0.1

Appendix G
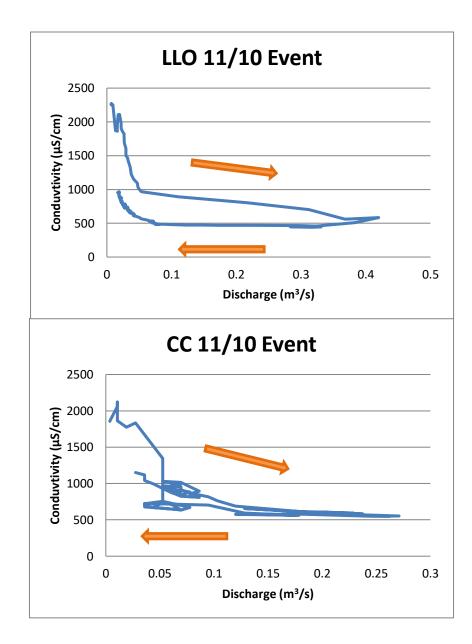
Cation Correlation with Impervious Surface

Stream Na vs Impervious Surface

R² = 0.9156

Stream Ca vs Impervious Surface

R² = 0.957

Stream Mg vs Impervious Surface

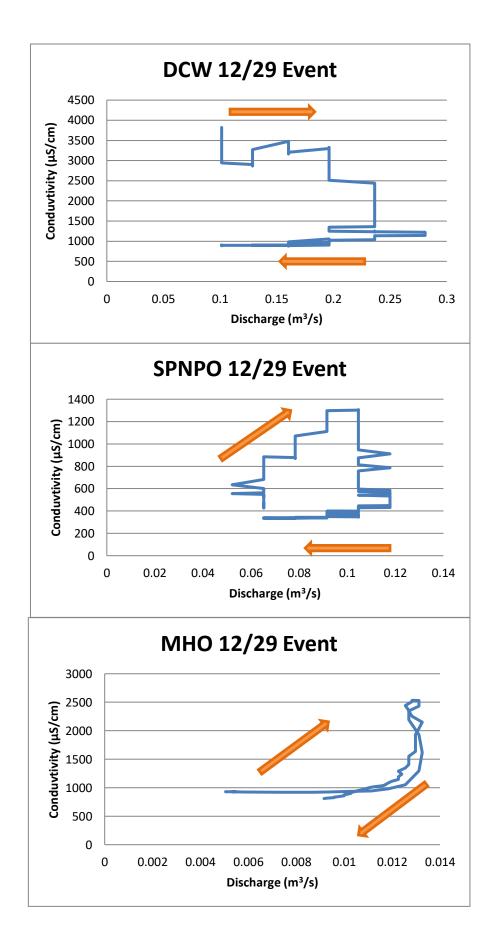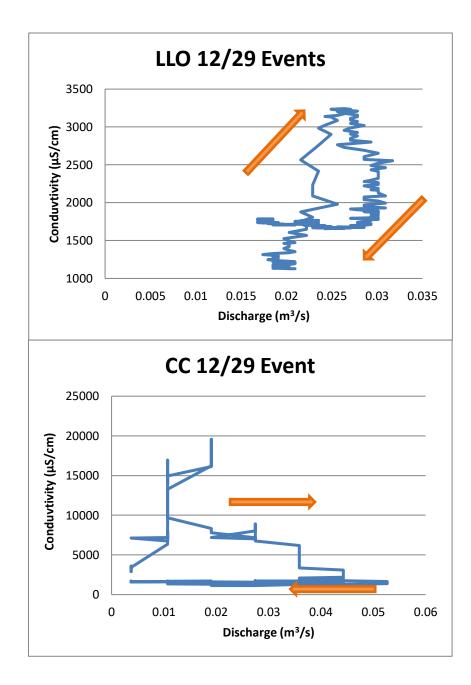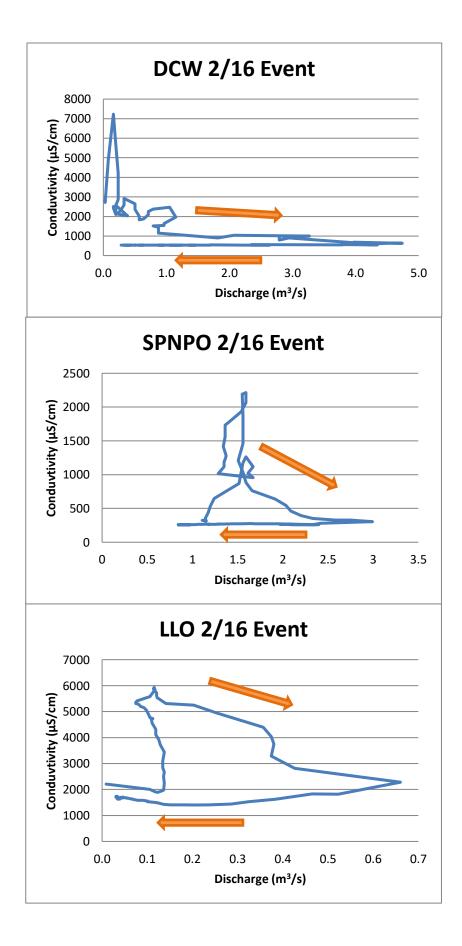R² = 0.9641

Stream K vs Impervious Surface

R² = 0.9375

Appendix H

Concentration/Discharge Hysteresis

DCW 11/10 Event

SPNPO 11/10 event

MHO 11/10 Event

LLO 11/10 Event

CC 11/10 Event

DCW 12/29 Event

SPNPO 12/29 Event

MHO 12/29 Event

LLO 12/29 Events

CC 12/29 Event

DCW 2/16 Event

SPNPO 2/16 Event

LLO 2/16 Event

CC 2/16 Event
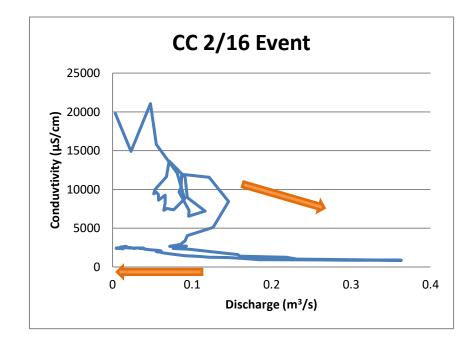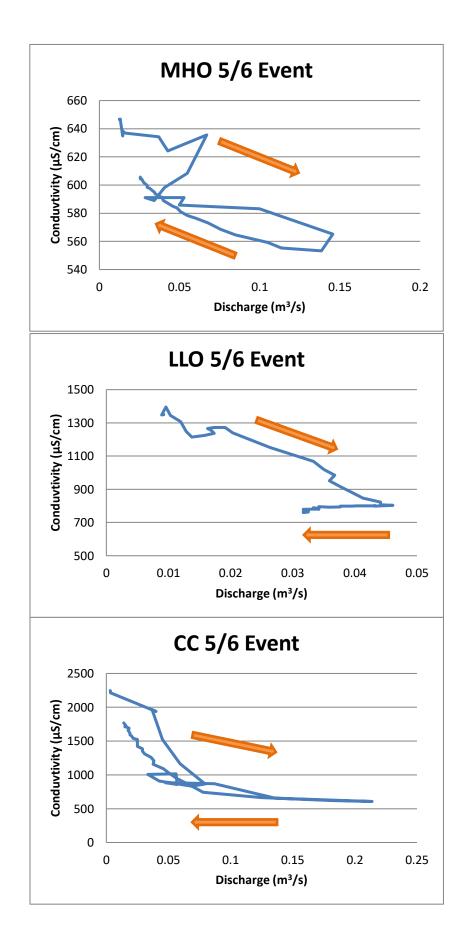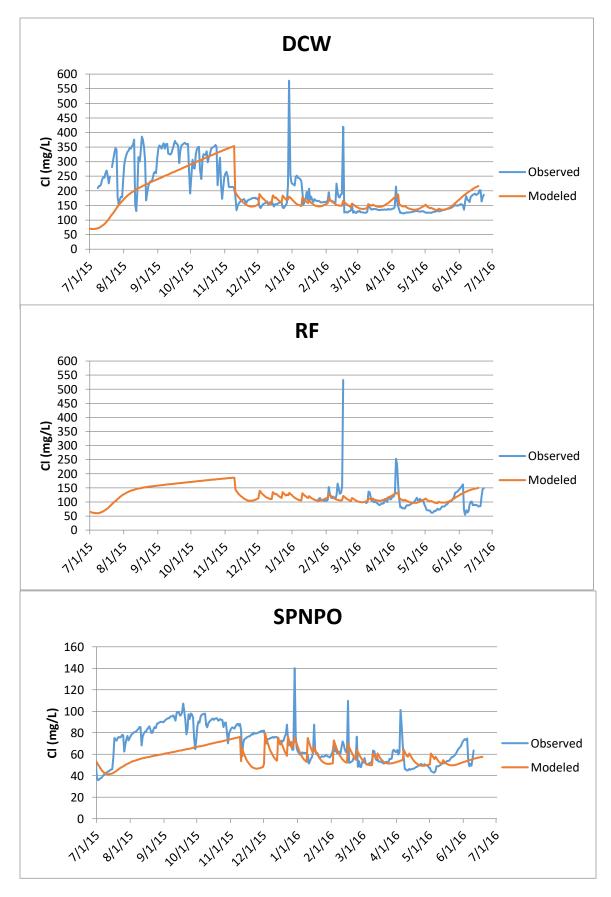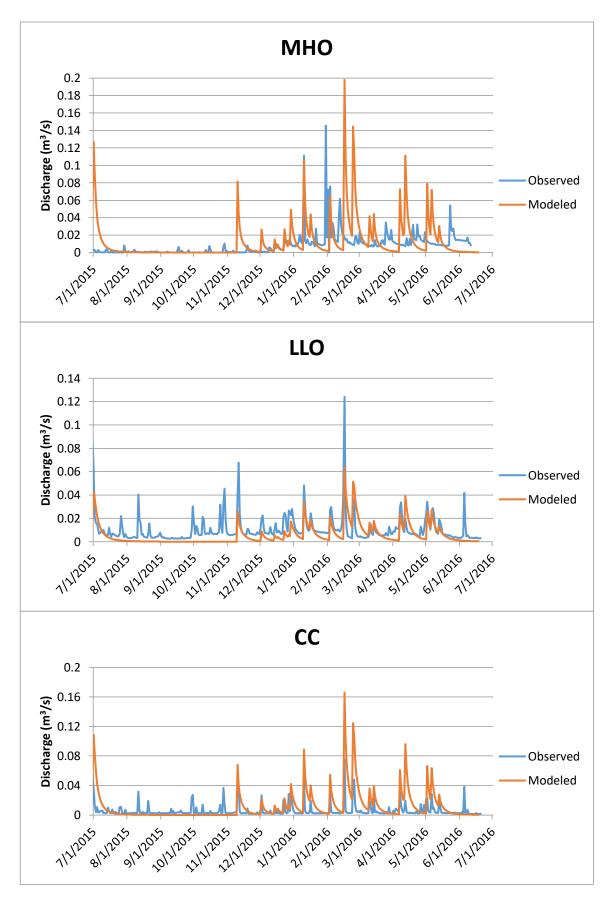
Appendix I

INCA-Cl Model Results

DCW Cl Load

RF Cl Load

SPNPO Cl Load

MHO Cl Load

LLO Cl load

CC Cl Load

DCW- Cl r²

MHO- Cl r²

R² = 0.3525

R² = 0.014

RF- Cl r²

LLO- Cl r²

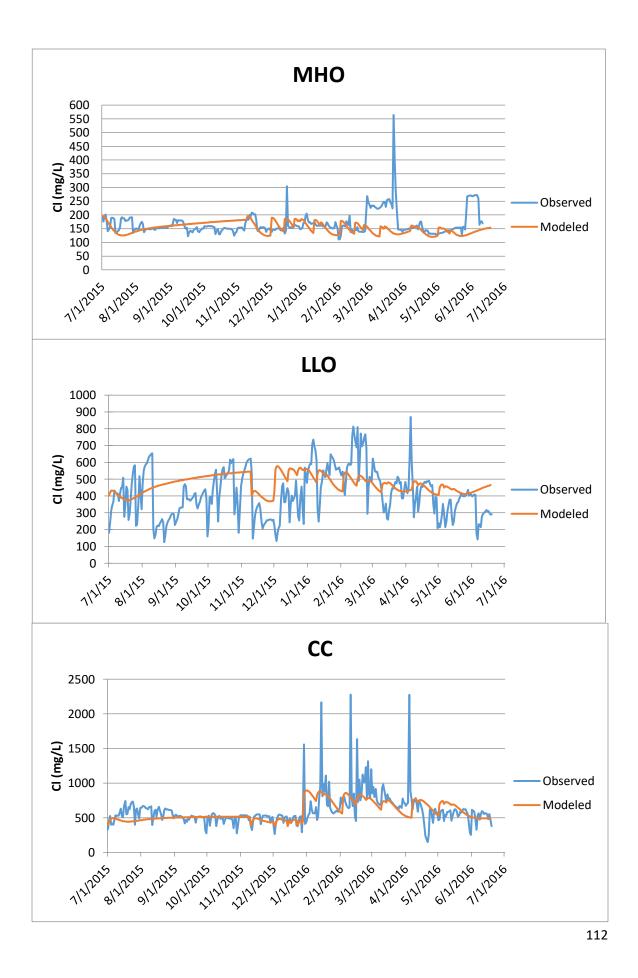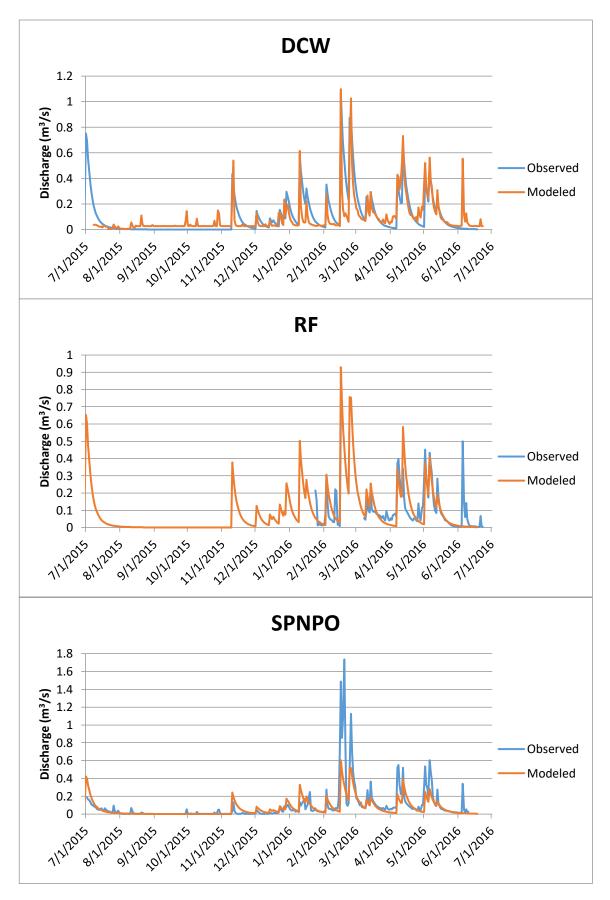R² = 0.054

R² = 0.0322

SPNPO- Cl r²

SPNPO- Cl r²

R² = 0.2404

R² = 0.1985

DCW- Discharge r^2

$R^2 = 0.6604$

MHO- Discharge r^2

$R^2 = 0.0389$

RF- Discharge r^2

$R^2 = 0.5594$

LLO- Discharge r^2

$R^2 = 0.2672$

SPNPO- Discharge r^2

$R^2 = 0.5801$

CC- Discharge r^2

$R^2 = 0.3107$

References

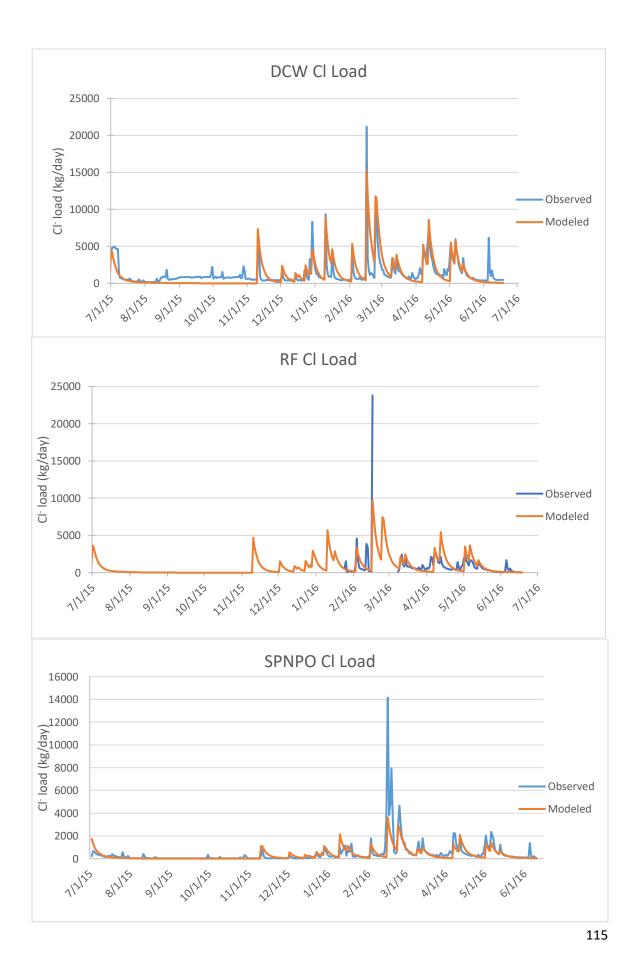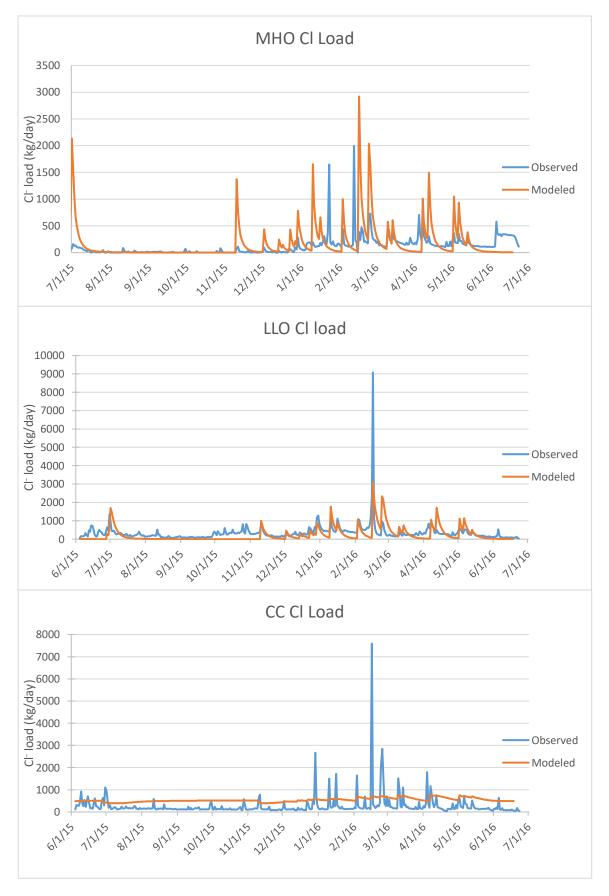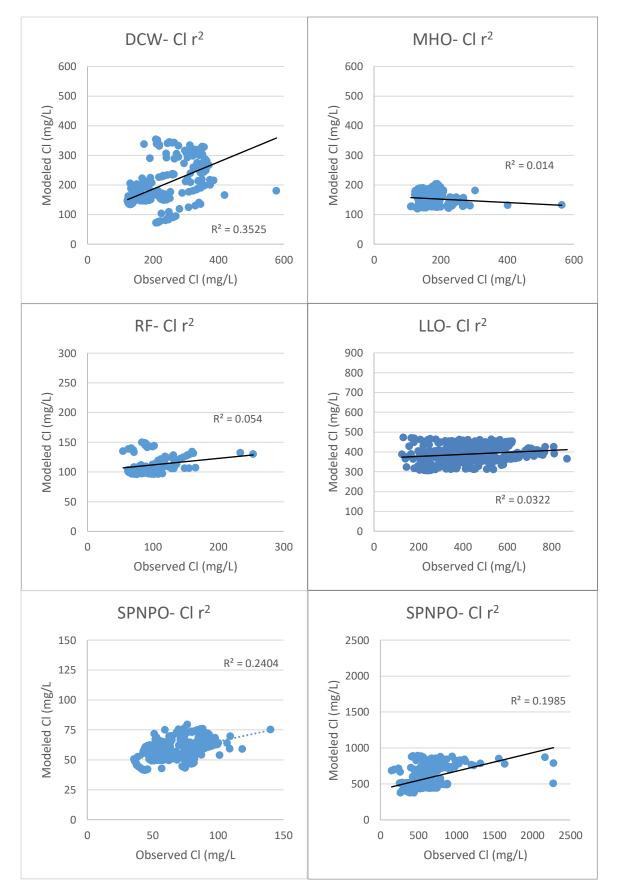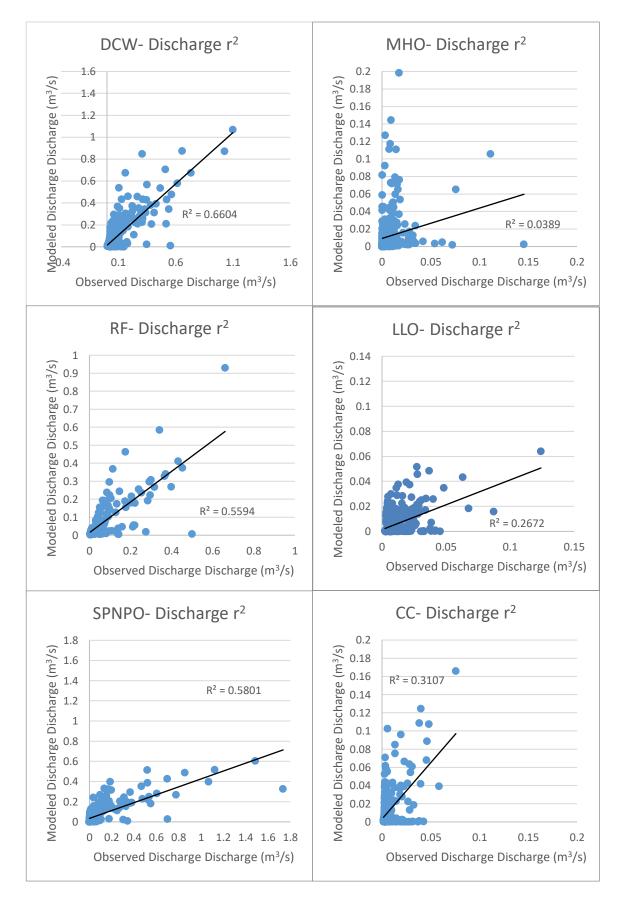Amrhein, Christopher, James E. Strong, and Paul A. Mosher. "Effect of deicing salts on metal and organic matter mobilization in roadside soils." *Environmental Science & Technology* 26.4 (1992): 703-709.

Allen, Richard G., Luis S. Pereira, Dirk Raes, and Martin Smith. "Crop evapotranspiration-Guidelines for computing crop water requirements-FAO Irrigation and drainage paper 56." *FAO, Rome* 300.9 (1998): D05109.

Corsi, Steven R., Laura A. De Cicco, Michelle A. Lutz, and Robert M. Hirsch. "River chloride trends in snow-affected urban watersheds: increasing concentrations outpace urban growth rate and are common among all seasons." Science of the Total Environment 508 (2015): 488-497.

Daley, Michelle L., Jody D. Potter, and William H. McDowell. "Salinization of urbanizing New Hampshire streams and groundwater: effects of road salt and hydrologic variability." *Journal of the North American Benthological Society* 28.4 (2009): 929-940.

Evans, Christopher, and Trevor D. Davies. "Causes of concentration/discharge hysteresis and its potential as a tool for analysis of episode hydrochemistry." *Water Resources Research* 34.1 (1998): 129-137.

Gburek, W. J., B. A. Needelman, and M. S. Srinivasan. "Fragipan controls on runoff generation: Hydropedological implications at landscape and watershed scales." *Geoderma* 131.3-4 (2006): 330-344.

Graney, Joseph, Karen Salvage, and Weixing Zhu. "A Watershed-Based Approach to Environmental Education Integrating Ecology, Hydrology, and Geochemistry." *Journal of Contemporary Water Research & Education* 138.1 (2008): 22-28.

Gutchess, Kristina, Li Jin, Laura Lautz, Stephen B. Shaw, Xiaoli Zhou, and Zunli Lu. "Chloride sources in urban and rural headwater catchments, central New York." *Science of the Total Environment* 565 (2016): 462-472.

Gutchess, Kristina, Li Jin, José LJ Ledesma, Jill Crossman, Christa Kelleher, Laura Lautz, and Zunli Lu. "Long-Term Climatic and Anthropogenic Impacts on Streamwater Salinity in New York State: INCA Simulations Offer Cautious Optimism." *Environmental Science & Technology* 52.3 (2018): 1339-1347.

Hayashi, Masaki. "Temperature-electrical conductivity relation of water for environmental monitoring and geophysical data inversion." *Environmental Monitoring and Assessment* 96.1-3 (2004): 119-128.

Heisig, Paul M. Effects of residential and agricultural land uses on the chemical quality of baseflow of small streams in the Croton Watershed, southeastern New York. No. 99-4173. US Geological Survey, 2000.

Horton, John D., Carma A. San Juan, and Douglas B. Stoeser. The State Geologic Map Compilation (SGMC) geodatabase of the conterminous United States. No. 1052. US Geological Survey, 2017.

Jackson, Robert B., and Esteban G. Jobbagy. "From icy roads to salty streams." *Proceedings of the National Academy of Sciences of the United States of America* 102.41 (2005): 14487-14488.

Jin, Li, Paul Whitehead, Donald I. Siegel, and Stuart Findlay. "Salting our landscape: An integrated catchment model using readily accessible data to assess emerging road salt contamination to streams."*Environmental Pollution* 159.5 (2011): 1257-1265

Johnson, Jason D., Joseph R. Graney, Rosemary C. Capo, and Brian W. Stewart. "Identification and quantification of regional brine and road salt sources in watersheds along the New York/Pennsylvania border, USA." *Applied Geochemistry 60* (2015): 37-50

Kaushal, Sujay S., Peter M. Groffman, Gene E. Likens, Kenneth T. Belt, William P. Stack, Victoria R. Kelly, Lawrence E. Band, and Gary T. Fisher. "Increased salinization of fresh water in the northeastern United States." *Proceedings of the National Academy of Sciences of the United States of America* 102.38 (2005): 13517-13520.

Kaushal, Sujay S. "Increased salinization decreases safe drinking water." *Environmental Science & Technology* 50.6 (2016): 2765-2766.

Kaushal, Sujay S., Shuiwang Duan, Thomas R. Doody, Shahan Haq, Rose M. Smith, Tamara A. Newcomer Johnson, Katie Delaney Newcomb, Julia Gorman, Noah Bowman, Paul M. Mayer, Kelsey L. Wood, Kenneth T. Belt, William P. Stack. "Human-accelerated weathering increases salinization, major ions, and alkalinization in fresh water across land use." *Applied geochemistry* 83 (2017): 121-135.

Kelly, Victoria R., Gary M. Lovett, Kathleen C. Weathers, Stuart EG Findlay, David L. Strayer, David J. Burns, and Gene E. Likens. "Long-term sodium chloride retention in a rural watershed: legacy effects of road salt on streamwater concentration." *Environmental Science & technology* 42.2 (2007): 410-415.

Kelly, Walton R. "Long-Term Trends in Chloride Concentrations in Shallow Aquifers near Chicago." *Groundwater* 46.5 (2008): 772-781.

Kincaid, Dustin W., and Stuart EG Findlay. "Sources of elevated chloride in local streams: groundwater and soils as potential reservoirs." *Water, Air, and Soil Pollution* 203.1-4 (2009): 335-342.

Klein, Richard D. "Urbanization and stream quality impairment." *JAWRA Journal of the American Water Resources Association* 15.4 (1979): 948-963.

Kuemmel, David A., and Rashad M. Hanbali. "Accident analysis of ice control operations." *Public Works* 124.8 (1993).

Lee, Jun Ho, and Ki Woong Bang. "Characterization of urban stormwater runoff." *Water Research* 34.6 (2000): 1773-1780.

Ledford, Sarah H., Laura K. Lautz, and John C. Stella. "Hydrogeologic processes impacting storage, fate, and transport of chloride from road salt in urban riparian aquifers." Environmental science & technology 50.10 (2016): 4979-4988.

Limbrick, K. J. "Estimating daily recharge to the Chalk aquifer of southern England? a simple methodology." *Hydrology and Earth System Sciences Discussions* 6.3 (2002): 485-496.

Long, David T., Thomas C. Voice, Irene Xagaroraki, Ao Chen, Huiyun Wu, Eunsang Lee, Amira Oun, and Fangli Xing. "Patterns of cq hysteresis loops and within an integrative pollutograph for selected inorganic and organic solutes and E. coli in an urban salted watershed during winter-early spring periods." *Applied Geochemistry* 83 (2017): 93-107.

Meriano, Mandana, Nick Eyles, and Ken WF Howard. "Hydrogeological impacts of road salt from Canada's busiest highway on a Lake Ontario watershed (Frenchman's Bay) and lagoon, City of Pickering." *Journal of Contaminant Hydrology* 107.1 (2009): 66-81.

McCann, John William. "Cumulative impacts of highly variable land-use within a New York watershed." *State University of New York at Binghamton Masters Thesis*, 2013.

National Research Council (US). Committee on the Comparative Costs of Rock Salt, and Calcium Magnesium Acetate (CMA) for Highway Deicing. *Highway deicing: comparing salt and calcium magnesium acetate*. No. 235. Transportation Research Board, 1991.

Novotny, Eric V., Andrew R. Sander, Omid Mohseni, and Heinz G. Stefan. "Chloride ion transport and mass balance in a metropolitan area using road salt." *Water Resources Research* 45.12 (2009): W12410

Perera, Nandana, Bahram Gharabaghi, and Ken Howard. "Groundwater chloride response in the Highland Creek watershed due to road salt application: A re-assessment after 20 years." *Journal of Hydrology* 479 (2013): 159-168.

Rantz, Saul Edward. *Measurement and computation of streamflow: volume 2, computation of discharge*. No. 2175. USGPO, 1982.

Rhodes, Amy L., Robert M. Newton, and Ann Pufall. "Influences of land use on water quality of a diverse New England watershed." *Environmental Science & Technology* 35.18 (2001): 3640-3645.

Rose, Seth. "Comparative solute–discharge hysteresis analysis for an urbanized and a 'control basin'in the Georgia (USA) Piedmont." *Journal of Hydrology* 284.1-4 (2003): 45-56.

Sheeder, Scott A., Jeremy D. Ross, and Toby N. Carlson. "Dual urban and rural hydrograph signals in three small watersheds." *JAWRA Journal of the American Water Resources Association* 38.4 (2002): 1027-1040.

Shanley, James B. "Effects of ion exchange on stream solute fluxes in a basin receiving highway deicing salts." *Journal of Environmental Quality* 23.5 (1994): 977-986.

Shaw, Stephen B., Rebecca D. Marjerison, David R. Bouldin, Jean-Yves Parlange, and M. Todd Walter. "Simple model of changes in stream chloride levels attributable to road salt applications." Journal of Environmental Engineering 138.1 (2011): 112-118.

Strahler, Arthur N. "Quantitative analysis of watershed geomorphology." Eos, Transactions American Geophysical Union 38.6 (1957): 913-920.

Sun, Hongbing, Maria Huffine, Jonathan Husch, and Leeann Sinpatanasakul. "Na/Cl molar ratio changes during a salting cycle and its application to the estimation of sodium retention in salted watersheds."*Journal of Contaminant Hydrology* 136 (2012): 96-105.

Wang, Kejin, Daniel E. Nelsen, and Wilfrid A. Nixon. "Damaging effects of deicing chemicals on concrete materials." *Cement and Concrete Composites*28.2 (2006): 173-188.

Whitehead, Paul G., E. J. Wilson, and D. Butterfield. "A semi-distributed Integrated Nitrogen model for multiple source assessment in Catchments (INCA): Part I—model structure and process equations." *Science of the Total Environment* 210 (1998): 547-558.

Zhu, Weixing, Joseph Graney, and Karen Salvage. "Land-use impact on water pollution: Elevated pollutant input and reduced pollutant retention."*Journal of Contemporary Water Research & Education* 138.1 (2008): 15-21.